Electronic Supplementary Material (ESI) for RSC Advances.

Supporting Information

Synthesis, characterization, TDDFT calculation and biological activity of tetradentate ligand based square pyramidal Cu(II)complexes

Apurba Bhunia,[a] Soumen Manna,[a] Soumen Mistri,[a] Aparup Paul,[a] Rajesh Kumar Manne,[b] Manas Kumar Santra,[b] Valerio Bertolasi,[c] Subal Chandra Manna*,[a]

[a]*Department of Chemistry and Chemical Technology, Vidyasagar University, Midnapore 721102, West Bengal, India, E-mail: scmanna@mail.vidyasagar.ac.in, Fax: (91) (03222) 275329.*

[b] *National Centre for Cell Science, NCCS Complex, Pune University Campus Ganeshkhind, Pune-411 007, Maharashtra, India.*

[c]*Dipartimento di Scienze Chimiche e Farmaceutiche, Centro di Strutturistica Diffrattometrica, Università di Ferrara, Via L. Borsari, 46, 44100 Ferrara, Italy.*

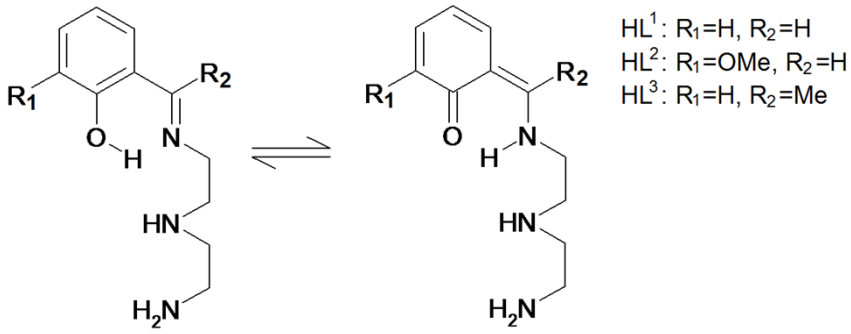

Chart 1S

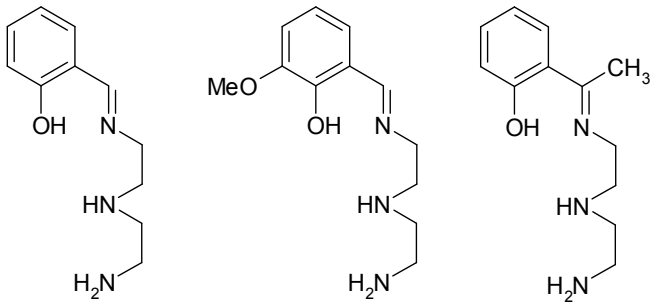

HL[1] **HL[2]** **HL[3]**

Chart 2S

Synthesis and characterization ligands

The ligands *o*-{[2-(2-aminoethylamino)ethylimino]methyl}phenol (HL^1), 2-{[2-(2-aminoethylamino)ethylimino]methyl}-6-methoxyphenol (HL^2) and *o*-{1-[2-(2-aminoethylamino)ethylimino]ethyl}phenol (HL^3) were prepared by condensation reaction of diethylenetriamine and related aldehydes / ketones.

HL[1]. A methanolic solution (10 mL) of diethylenetriamine (10 mmol, 1.03 g) was added drop wise to a methanolic solution (10 mL) of 2-hydroxybenzaldehyde (10 mmol, 1.22 g) with constant stirring. Resulting yellow reaction mixture was stirred for 3 h and a brown colour compound separated out and filtered. Brown compound was re-dissolved in methanol and filtered; the filtrate was kept for crystallization under slow evaporation conditions at room temperature. Crystalline solid was collected by filtration and dried in air to afford HL^1 as a deep brown solid. Yield: 1.759g (85 %). $C_{11}H_{17}N_3O$ (207): C, 63.76; H, 8.21; N, 20.28%. Found: C, 63.74; H, 8.22; N, 20.29 (%). FT-IR (KBr), cm^{-1}: 3200-3600 (br,vs), 2982 (s), 2944 (s), 1633 (vs), 1557 (vs), 1496 (s), 1465 (s), 1414 (vs), 1373 (s), 1300 (s), 1280 (s), 1151 (w), 1078 (w), 881 (w), 817 (s), 756 (s), 640 (s). ^1H NMR ($CDCl_3$, 200 MHz, δ, ppm): 8.35 s (1H), 7.34-7.20 m (2H), 6.97-6.81 m (2H), 4.67 s (1H), 3.72 s (3H), 3.02-2.64 m (8H).

HL²and **HL³.**Brown colour ligands were synthesized adopting the same procedure as HL^1, using 2-hydroxy-3-methoxybenzaldehyde (10 mmol, 1.52 g) and 2′-hydroxyacetophenone (10 mmol, 1.36 g) for ligands HL^2 and HL^3, respectively, instead of using 2-hydroxybenzaldehyde. For HL^2: Yield: 1.943g (82 %). $C_{12}H_{19}N_3O_2$ (237) : C, 60.75; H, 8.01; N, 17.72 %. Found: C, 60.73; H, 8.02; N, 17.73 (%). FT-IR (KBr), cm^{-1}: 3200-3600 (br,vs), 2943 (s), 2839 (s), 1642 (vs), 1542 (vs), 1506 (vs), 1467 (vs), 1411 (s), 1252 (vs), 1227 (vs), 1169 (s), 1081 (s), 964 (s), 847 (s), 783 (s), 739 (s), 621 (s). ^{1}H NMR ($CDCl_3$, 200 MHz, δ, ppm): 8.36 s (1H), 6.95-6.75 m (3H), 4.77 s (1H), 4.01-3.73 m (3H), 3.85 s (3H), 3.01-2.72 m (8H). For HL^3: Yield: 1.657g (75 %). $C_{12}H_{19}N_3O$ (221): C, 65.15; H, 8.59; N, 19.00 %. Found: C, 65.13; H, 8.58; N, 19.00 (%). FT-IR (KBr), cm^{-1}: 3200-3600 (br,vs), 2978(s), 2952 (s), 1643 (vs), 1551 (vs), 1487 (s), 1467 (s), 1413 (s), 1372 (s), 1301 (s), 1079 (w), 881 (w), 820 (s), 664 (s). ^{1}H NMR ($CDCl_3$, 200 MHz, δ, ppm): 7.56 - 7.49 m (1H), 7.30 - 7.27 m (1H), 6.96 - 6.90 m (1H), 6.83 - 6.80 m (1H), 4.78 s (1H), 3.73 t (J= 6.0 H_Z, 2H), 3.12 - 3.02 m (3H), 2.86 - 2.70 m (6H), 2.39 s (3H).

Infrared spectral studies

The most important absorption bands in IR spectroscopy of complexes are summarized in experimental section and tabulated in Table 14S. The spectra (Figs. 26S-28S) of complexes exhibit that ν_s(C-O) for **1** and **3** appear at 1300 cm^{-1} while that for **2** appear at 1297 cm^{-1}.Aromatic ν(C=C, C=N) stretching vibrations for **1**, **2** and **3** appear in the region 1372-1649 cm^{-1}, 1372-1639 cm^{-1} and 1372-1643 cm^{-1}, respectively. The bands in the region 2972-2982 cm^{-1} corresponds to the aromatic ν(C-H) stretching vibrations. The spectra of complexes **1**, **2** and **3** show broad bands in the region 3190-3500 cm^{-1}, which are assigned to the ν(O–H) stretching

vibrations of water molecules.[£] Aliphatic $\nu(C_{sp3}\text{-}H)$ stretching vibration for all complexes appear at 2943 cm^{-1}. Stretching vibration of perchlorate anions appear in the region 1072-1124 cm^{-1}. The IR spectra of complexes also show bands corresponding to $\rho_w(H_2O)$ [515 cm^{-1} for **1** and **2**, 551 cm^{-1} for **3**].

[£]K. Nakamoto, *Infrared Spectra of Inorganic and Coordination Compounds*, John Wiley & Sons, New York, 1997.

Table 1S. Experimental and calculated[e] coordination bond lengths (Å) and angles (°) and τ_5 parameter for complexes **1-3,** using B3LYP, B3PW91 and MPW1PW91 functionals.

Complex	Parameters	Exp	Calcd		
			B3LYP	B3PW91	MPW1PW91
1	Bond lengths				
	Cu1- O1	1.922(2)	1.940	1.933	1.926
	Cu1-O2	2.394(2)	2.328	2.328	2.307
	Cu1- N1	1.939(2)	1.977	1.965	1.965
	Cu1-N2	2.009(2)	2.061	2.047	2.042
	Cu1-N3	2.010(3)	2.065	2.053	2.048
	Bond angles				
	O1 -Cu1-O2	96.40(1)	100.86	100.65	100.65
	O1-Cu1-N1	94.20(1)	93.62	93.72	93.64
	O1 -Cu1-N2	172.90(1)	172.83	173.05	172.59
	O1 -Cu1-N3	95.00(1)	94.71	94.41	94.43
	O2 -Cu1-N1	101.80(1)	98.50	98.30	98.07
	O2 -Cu1-N2	90.70(1)	86.28	86.28	86.73
	O2 -Cu1-N3	89.10(1)	96.28	96.39	96.59
	N1 -Cu1-N2	84.60(1)	84.71	84.85	84.78
	N1-Cu1 -N3	164.90(1)	161.32	161.57	161.63
	N2 -Cu1-N3	84.70(1)	84.94	85.06	85.09

	τ_5 parameter	0.133	0.191	0.191	0.182
2	Bond lengths				
	Cu1- O1	1.908(3)	1.940	1.933	1.926
	Cu1-O2	2.428(3)	2.330	2.328	2.311
	Cu1- N1	1.935(6)	1.973	1.962	1.961
	Cu1-N2	2.029(4)	2.060	2.048	2.042
	Cu1-N3	1.988(5)	2.062	2.050	2.045
	Bond angles				
	O1 -Cu1-O2	90.22(12)	100.71	100.60	100.67
	O1-Cu1-N1	94.61(18)	93.39	93.40	93.41
	O1 -Cu1-N2	178.26(14)	173.09	173.09	172.82
	O1 -Cu1-N3	96.02(18)	94.85	94.72	94.61
	O2 -Cu1-N1	107.66(14)	98.64	98.56	98.13
	O2 -Cu1-N2	88.40(14)	86.15	86.27	86.47
	O2 -Cu1-N3	90.94(15)	96.25	96.25	96.34
	N1 -Cu1-N2	84.80(2)	84.81	84.85	84.86
	N1-Cu1 -N3	158.52(17)	161.30	161.47	161.83
	N2 -Cu1-N3	85.10(2)	84.98	85.09	85.14
	τ_5 parameter	0.329	0.196	0.193	0.183
3	Bond lengths				
	Cu1- O1	1.862(3)	1.911	1.905	1.900
	Cu1-O2	2.465(3)	2.353	2.354	2.332
	Cu1- N1	1.924(3)	1.994	1.982	1.980
	Cu1-N2	1.960(3)	2.041	2.028	2.024
	Cu1-N3	2.029(4)	2.073	2.061	2.056

	Bond angles				
	O1 -Cu1-O2	94.90(1)	100.54	100.42	100.32
	O1-Cu1-N1	89.00(1)	93.72	93.84	93.76
	O1 -Cu1-N2	176.80(2)	173.45	173.63	173.47
	O1 -Cu1-N3	99.50(1)	93.60	93.41	93.46
	O2 -Cu1-N1	102.30(1)	96.13	95.81	95.87
	O2 -Cu1-N2	88.10(1)	85.94	85.87	86.15
	O2 -Cu1-N3	88.40(2)	96.52	96.61	96.52
	N1 -Cu1-N2	91.40(2)	86.33	86.39	86.32
	N1-Cu1 -N3	165.80(2)	163.95	164.22	164.28
	N2 -Cu1-N3	79.50(2)	84.77	84.85	84.92
	τ_5 parameter	0.183	0.158	0.156	0.153

[e]Using conductor-like polarizable continuum model (CPCM) in methanol; basis set, LanL2DZ.

Table 2S. Hydrogen bond parameters (Å, °) for complexes **1**, **2** and **3**.

	D-H…A	*d*(D-H)	*d*(D…A)	*d*(H…A)	<(D-H…A)	Symmetry code A
Complex **1**	N(2)-H(2N)…O(3)	0.890(1)	3.076(4)	2.280(2)	148(1)	x,y,z
	N(3)-H(2N3)…O(2)	0.900(4)	3.159(3)	2.540(4)	126(3)	-x,1-y,-z
	O(2)-H(1O2)…O(1)	0.940(3)	2.745(3)	1.960(3)	140(2)	-x,1-y,-z
	N (3)-H(1N3)…O(5)	0.900(2)	3.108(5)	2.430(3)	133(1)	-x,y-1/2,1/2-z
	O(2)-H(2O2)…O (4)	0.940(3)	3.032(4)	2.180(3)	151(2)	x,3/2-y,z-1/2
Complex **2**	N(2)-H(2N)…O(3)	0.895(12)	3.054(6)	2.200(2)	160(5)	x,y,z
	O(2)-H(2O2)…O(4)	0.940(6)	2.897(9)	1.960(6)	176(6)	x,y,z
	N(3)-H(2N3)…O(7)	0.894(1)	3.275(5)	2.520(4)	142(6)	x-y, -y,2/3-z
	N(3)-H(2N3)…O(1)	0.890(1)	3.366(5)	2.660(4)	136(1)	x-y, -y,2/3-z
	O(2)-H(1O2)…O(7)	0.940(3)	3.031(5)	2.400(5)	124(6)	y+1,x-1,1-z
	N(3)-H(1N3)…O(2)	0.890(5)	3.046(6)	2.230(4)	152(4)	y+1,x-1,1-z
	O(2)-H(1O2)…O(1)	0.940(3)	2.884(5)	1.980(5)	160(5)	y+1,x-1,1-z
Complex **3**	N(2)-H(2N)…O(3)	0.900(2)	3.004(7)	2.210(4)	148(1)	x,y,z
	O(2)-H(1O2)…O(4)	0.950(5)	3.183(8)	2.580(6)	122(4)	x,y,z
	N(3)-H(1N3)…O(1)	0.900(4)	3.336(5)	2.470(4)	160(3)	1-x,1-y,1-z
	O(2)-H(2O2)…O(1)	0.940(4)	2.692(4)	1.880(3)	143(3)	1-x,1-y,1-z
	N(3)-H(2N3)…O(4)	0.900(2)	3.015(9)	2.200(3)	152(2)	1-x,y-1/2,1/2-z
	O(2)-H(2O2)…O(6)	0.950(5)	3.273(6)	2.600(5)	128(4)	x,3/2-y,1/2+z

Table 3S. C-H···π interaction parameters in complexes **1**, **2** and **3**.

Complex	C−H (I)	C−H (I)→ C_g(J)	H···C_g(4) (Å)	<C−H···C_g (°)	C···C_g(Å)
1	C(9)–H(9A)	[1] → C_g(4)	2.73	165	3.680
2	C(9)–H(9A)	[1] → C_g(4)	2.64	164	3.577
	C(12) –H(12A)	[1] → C_g(4)	2.85	141	3.646
3	C(10) –H(10A)	[1] → C_g(4)	2.76	166	3.710
	C(8)-H(8A)	[1] → C_g(4)	3.14	124	3.772

C_g(4) = (C1-C2-C3-C4-C5-C6)

Table 4S. Comparative data table of complex **1** and two related reported structure, having same cationic unit.

Complex	$[Cu(L^1)(H_2O)]\cdot ClO_4$ (Complex **1**)	$[Cu(L^1)(H_2O)]\cdot Cl$[31a]	$[Cu(L^1)(H_2O)]\cdot PF_6$[31b]
Deviation of central atom from mean plane formed by four equatorial coordinated atoms.	0.1577 Å	0.1785 Å	0.1763 Å
τ parameter	0.133	0.196	0.142

Table 5S. Calculated (using B3LYP functional) list of excitation energies of complexes **1, 2** and **3** in methanolic solution.

Complex	Excitation	Wavelength λ (nm)	Oscillatory strength (*f*)	Major Contribution	Assignment[f]
	1	711.44	0.0004	HOMO -3(β) →LUMO (β) (23%), HOMO (β) → LUMO (β) (60%)	IMCT LMCT$^{\delta}$
	2	580.69	0.0003	HOMO -3(β) →LUMO (β) (44%)	IMCT
	3	512.03	0.0112	HOMO -10(β) →LUMO (β) (27%),	LMCT$^{\delta}$
				HOMO -7(β) →LUMO (β) (11%),	LMCT$^{\delta}$
				HOMO -6(β) →LUMO (β) (12%)	LMCT$^{\delta}$
	4	483.10	0.0064	HOMO -14(β) →LUMO (β)(17%), HOMO -11(β) →LUMO(β)(14%),	LMCT$^{\delta}$

			HOMO -9(β) →LUMO (β) (16%)	LMCT$^{\delta}$
				IMCT
6	432.67	0.0001	HOMO -8(β) →LUMO (β) (11%),	LMCT$^{\Lambda}$
			HOMO (β) →LUMO (β) (24%)	LMCT$^{\delta}$
8	364.07	0.0508	HOMO -1(α) →LUMO (α) (11%),	ILCT$^{\theta}$
			HOMO (α) →LUMO (α) (36%),	ILCT$^{\theta}$
			HOMO (β) →LUMO+1(β) (36%)	ILCT$^{\theta}$
9	359.35	0.0097	HOMO -1(α) →LUMO (α) (81%)	ILCT$^{\theta}$
10	337.57	0.0029	HOMO -1(β) →LUMO (β) (77%)	LMCT$^{\delta}$
11	318.10	0.1704	HOMO -2(β) →LUMO (β) (50%)	LMCT$^{\delta}$
14	270.50	0.1498	HOMO -4(β) →LUMO (β) (33%)	LMCT$^{\delta}$
15	260.20	0.2766	HOMO -2(α) →LUMO (α) (20%),	ILCT$^{\theta}$
			HOMO -4(β) →LUMO (β) (12%),	LMCT$^{\delta}$
			HOMO -1(β) →LUMO+1(β) (17%)	ILCT$^{\theta}$
19	243.92	0.0455	HOMO (α) →LUMO+1(α) (19%),	ILCT$^{\theta}$
			HOMO -7(β) →LUMO (β) (18%)	LMCT$^{\delta}$
24	232.13	0.0563	HOMO (α) →LUMO+2(α) (22%)	LMCT$^{\delta}$
27	229.36	0.0009	HOMO -1(α) →LUMO+1(α) (56%)	ILCT$^{\theta}$
28	228.31	0.0053	HOMO (α) →LUMO+3(α) (63%),	LMCT$^{\delta}$
			HOMO (β) →LUMO+4(β) (12%)	LMCT$^{\delta}$
31	222.10	0.0003	HOMO -1(α) →LUMO+1(α) (10%),	ILCT$^{\theta}$
			HOMO -1(α) →LUMO+2(α) (82%)	LMCT$^{\delta}$
32	221.09	0.0002	HOMO -11(β) →LUMO (β) (39%),	LMCT$^{\delta}$
			HOMO -8(β) →LUMO (β) (11%)	LMCT$^{\Lambda}$
33	219.96	0.0017	HOMO -7(β) →LUMO (β) (25%)	LMCT$^{\delta}$
36	214.66	0.0007	HOMO -1(α) → LUMO+3(α) (78%)	LMCT$^{\delta}$

	38	213.16	0.0326	HOMO -5(α) →LUMO (α) (20%),	ILCT$^{\theta}$
				HOMO -1(α) →LUMO+3(α) (12%),	LMCT$^{\delta}$
				HOMO (α) →LUMO+5(α) (14%)	ILCT$^{\theta}$
	39	211.52	0.0541	HOMO -13(β) →LUMO (β) (12%)	ILCT$^{\theta}$
	40	209.77	0.1642	HOMO -5(α) →LUMO (α) (21%)	ILCT$^{\theta}$
	41	204.90	0.0015	HOMO (β) →LUMO+7(β) (43%)	LMCT$^{\delta}$
	42	204.46	0.0017	HOMO -2(β) →LUMO+2(β) (50%),	ILCT$^{\theta}$
				HOMO (β) →LUMO+7(β) (13%)	LMCT$^{\delta}$
	43	203.46	0.0121	HOMO (α) →LUMO+6(α) (33%),	LMCT$^{\delta}$
				HOMO (β) →LUMO+7(β) (16%)	LMCT$^{\delta}$
	45	199.62	0.0035	HOMO -1(α) →LUMO+4(α) (71%)	LMCT$^{\delta}$
	47	196.77	0.0689	HOMO -6(α) →LUMO (α) (13%),	ILCT$^{\theta}$
				HOMO -1(α) →LUMO+4(α) (15%),	LMCT$^{\delta}$
				HOMO -1(α) →LUMO+5(α) (38%)	ILCT$^{\theta}$
	48	196.57	0.0915	HOMO -1(α) →LUMO+5(α) (30%)	ILCT$^{\theta}$
	49	195.81	0.0379	HOMO -1(β) →LUMO+2(β) (34%),	ILCT$^{\theta}$
				HOMO -1(β) →LUMO+3(β) (40%)	LMCT$^{\delta}$
2	1	747.78	0.0004	HOMO -3(β) → LUMO (β) (13%),	IMCT
				HOMO (β) → LUMO (β) (67%)	LMCT$^{\Gamma}$
	2	590.98	0.0003	HOMO -3(β) → LUMO (β) (53%)	IMCT
	4	512.77	0.0104	HOMO -11(β) → LUMO (β) (11%),	LMCT$^{\Gamma}$
				HOMO -9(β) → LUMO (β) (12%),	LMCT$^{\Gamma}$
				HOMO -4(β) → LUMO (β) (21%)	LMCT$^{\Gamma}$
	5	486.24	0.0088	HOMO -14(β) →LUMO (β) (14%),	LMCT$^{\Gamma}$
				HOMO -13(β) →LUMO (β) (14%),	IMCT
				HOMO -9(β) →LUMO (β) (13%),	LMCT$^{\Gamma}$

			HOMO -2(β) →LUMO (β) (17%)	LMCT$^{\Gamma}$
8	386.59	0.0592	HOMO (α) → LUMO (α) (42%),	ILCT$^{\Psi}$
			HOMO (β) →LUMO+1(β) (46%)	ILCT$^{\Psi}$
9	373.06	0.0063	HOMO -1(β) → LUMO (β) (69%)	LMCT$^{\Gamma}$
10	357.45	0.0006	HOMO -1(α) → LUMO (α) (88%)	ILCT$^{\Psi}$
12	320.46	0.1005	HOMO -2(β) → LUMO (β) (56%)	LMCT$^{\Gamma}$
13	284.16	0.3282	HOMO -2(α) → LUMO (α) (32%),	ILCT$^{\Psi}$
			HOMO -2(β) →LUMO+1(β)(12%),	ILCT$^{\Psi}$
			HOMO -1(β) →LUMO+1(β) (34%)	ILCT$^{\Psi}$
15	263.83	0.1572	HOMO -5(β) → LUMO (β) (27%),	LMCT$^{\Gamma}$
			HOMO -4(β) →LUMO (β) (18%)	LMCT$^{\Gamma}$
18	253.04	0.0520	HOMO (α) →LUMO+1(α) (67%),	LMCT$^{\Gamma}$
			HOMO (β) →LUMO+2(β) (21%)	LMCT$^{\Gamma}$
21	246.03	0.0458	HOMO -7(β) →LUMO (β) (52%)	LMCT$^{\Gamma}$
22	244.23	0.0034	HOMO -5(β) → LUMO (β) (24%),	LMCT$^{\Gamma}$
			HOMO (β) →LUMO+4(β) (17%)	LMCT$^{\Gamma}$
24	241.89	0.0300	HOMO (α) →LUMO +2(α) (10%),	ILCT$^{\Psi}$
			HOMO (α) →LUMO+3(α) (64%),	LMCT$^{\Gamma}$
			HOMO (β) →LUMO+4(β) (10%)	LMCT$^{\Gamma}$
27	232.29	0.1648	HOMO (α) →LUMO +2(α) (28%),	ILCT$^{\Psi}$
			HOMO (β) →LUMO+3(β) (24%)	ILCT$^{\Psi}$
28	231.00	0.0195	HOMO -10(β) →LUMO (β) (32%),	LMCT$^{\Lambda}$
			HOMO -6(β) →LUMO (β) (26%)	LMCT$^{\Gamma}$
31	226.78	0.0200	HOMO (α) →LUMO +4(α) (68%)	LMCT$^{\Gamma}$
33	224.03	0.1121	HOMO (α) →LUMO +5(α) (31%)	LMCT$^{\Gamma}$
34	222.67	0.0001	HOMO -1(α) →LUMO +1(α) (90%)	LMCT$^{\Gamma}$

	35	220.87	0.0001	HOMO -11(β) → LUMO (β) (26%),	LMCT$^{\Gamma}$
				HOMO -10(β) →LUMO (β) (19%),	LMCT$^{\Lambda}$
				HOMO -7(β) →LUMO (β) (10%)	LMCT$^{\Gamma}$
	36	220.61	0.0010	HOMO -8(β) → LUMO (β) (64%)	LMCT$^{\Gamma}$
	39	214.24	0.0008	HOMO -1(α) →LUMO +3(α) (85%)	LMCT$^{\Gamma}$
	41	212.12	0.0137	HOMO -6(α) →LUMO (α) (17%),	ILCT$^{\Psi}$
				HOMO -4(α) →LUMO (α) (11%),	ILCT$^{\Psi}$
				HOMO -14(β) →LUMO (β) (13%)	ILCT$^{\Psi}$
	42	211.72	0.0093	HOMO (α) →LUMO+6(α) (38%),	LMCT$^{\Gamma}$
				HOMO (β) →LUMO+7(β) (16%)	LMCT$^{\Gamma}$
	43	209.40	0.0171	HOMO -14(β) →LUMO (β) (15%)	LMCT$^{\Gamma}$
	45	206.87	0.0263	HOMO -2(α) →LUMO+1(α) (17%),	LMCT$^{\Gamma}$
				HOMO -1(β) →LUMO+2(β) (43%)	LMCT$^{\Gamma}$
	48	204.68	0.0085	HOMO -12(β) →LUMO (β) (53%),	LMCT$^{\Gamma}$
				HOMO -9(β) →LUMO (β) (25%)	LMCT$^{\Gamma}$
3	1	703.09	0.0008	HOMO-3(β) → LUMO (β) (19%),	IMCT
				HOMO (β) →LUMO (β) (63%)	LMCT$^{\Omega}$
	2	572.24	0.0009	HOMO -3(β) →LUMO (β) (49%)	IMCT
	3	499.28	0.0074	HOMO-9(β) → LUMO (β) (37%)	IMCT
	4	475.34	0.0082	HOMO-14(β) → LUMO (β) (15%),	LMCT$^{\Omega}$
				HOMO -13(β) →LUMO (β) 10%),	LMCT$^{\Omega}$
				HOMO -10(β) →LUMO (β) (25%)	LMCT$^{\Omega}$
	6	424.89	0.0001	HOMO-8(β) →LUMO (β)(12%),	LMCT$^{\Lambda}$
				HOMO (β) →LUMO(β) (22%)	LMCT$^{\Omega}$
	8	362.58	0.0466	HOMO-1(α) → LUMO (α) (23%),	ILCT$^{\Phi}$
				HOMO (α) →LUMO (α) (30%),	ILCT$^{\Phi}$

			HOMO (β) →LUMO+1(β) (32%)	ILCT$^{\Phi}$
9	353.62	0.0247	HOMO-1(α) → LUMO (α) (70%)	ILCT$^{\Phi}$
10	334.06	0.0016	HOMO-1(β) →LUMO (β) (74%)	LMCT$^{\Omega}$
11	318.90	0.1882	HOMO-2(β) →LUMO (β) (60%)	LMCT$^{\Omega}$
14	270.90	0.1228	HOMO -4(β) →LUMO (β) (34%),	LMCT$^{\Omega}$
16	257.24	0.2603	HOMO-2(α) → LUMO (α) (22%),	ILCT$^{\Phi}$
			HOMO -4(β) →LUMO (β) (16%),	LMCT$^{\Omega}$
			HOMO -1(β) →LUMO+1(β) (20%)	ILCT$^{\Phi}$
19	244.46	0.0734	HOMO (α) →LUMO+1(α) (16%)	LMCT$^{\Omega}$
			HOMO (β) →LUMO+2(β) (53%),	LMCT$^{\Omega}$
			HOMO (β) →LUMO+3(β) (10%)	ILCT$^{\Phi}$
27	230.04	0.0047	HOMO-1(α) →LUMO+1(α) (51%),	LMCT$^{\Omega}$
			HOMO -1(α) →LUMO+2(α) (14%)	ILCT$^{\Phi}$
28	228.65	0.0397	HOMO (α) →LUMO+3(α) (12%),	LMCT$^{\Omega}$
			HOMO (β) →LUMO+3(β) (13%)	ILCT$^{\Phi}$
31	223.50	0.0002	HOMO -1(α) →LUMO+2(α) (68%)	ILCT$^{\Phi}$
37	216.92	0.0126	HOMO-1(α) → LUMO+3(α) (55%)	LMCT$^{\Omega}$
40	210.54	0.0104	HOMO-5(α) → LUMO (α) (20%),	ILCT$^{\Phi}$
			HOMO -4(α) →LUMO (α) (19%)	ILCT$^{\Phi}$
42	206.36	0.0189	HOMO (α) →LUMO+6(α) (46%),	LMCT$^{\Omega}$
			HOMO (β) →LUMO+7(β) (26%)	LMCT$^{\Omega}$
44	202.09	0.0018	HOMO-1(α) →LUMO+4(α) (46%)	LMCT$^{\Omega}$
46	200.18	0.0049	HOMO-1(α) →LUMO+4(α) (47%)	LMCT$^{\Omega}$
			HOMO -1(α) →LUMO+5(α) (40%)	ILCT$^{\Phi}$
48	197.62	0.1405	HOMO-6(α) → LUMO (α) (27%),	ILCT$^{\Phi}$

				HOMO -2(α) →LUMO+1(α) (10%),	$LMCT^{\Omega}$
				HOMO -5(β) →LUMO+1(β) (11%)	$ILCT^{\Phi}$
	50	194.92	0.0146	HOMO -1(α) →LUMO+6(α) (74%)	$LMCT^{\Omega}$

[f]$ILCT^{\theta}$ = intra ligand charge transfer transition in L^1; $ILCT^{\psi}$= intra ligand charge transfer transitioninL^2 ; $ILCT^{\Phi}$ = intra ligand charge transfer transitionin L^3; $LMCT^{\delta}$= L^1 to metal charge transfer transition; $LMCT^{\Gamma}$= L^2 to metal charge transfer transition; $LMCT^{\Omega}$ = L^3 to metal charge transfer transition; $LMCT^{\Lambda}$ = water to metal charge transfer transition and IMCT = intra metal charge transfer transition.

Table 6S. List of selected excitation bands of complexes **1, 2** and **3** calculated in different functionals (B3LYP, B3PW91, MPW1PW91) in CPCM model in methanolic solution.

Complex	Functional	Wavelength λ(nm)	Oscillatory strength (*f*)	Major Contribution	Assignment[g]
1	B3LYP	512.03	0.0112	HOMO-10(β) →LUMO (β) (27%),	$LMCT^{\delta}$
				HOMO-7(β) →LUMO (β) (11%),	$LMCT^{\delta}$
				HOMO-6(β) →LUMO (β) (12%)	$LMCT^{\delta}$
		359.35	0.0097	HOMO -1(α) →LUMO (α) (81%)	$ILCT^{\theta}$
		318.10	0.1704	HOMO -2(β) →LUMO (β) (50%)	$LMCT^{\delta}$
		260.20	0.2766	HOMO -2(α) →LUMO (α) (20%),	$ILCT^{\theta}$
				HOMO -4(β) →LUMO (β) (12%),	$LMCT^{\delta}$
				HOMO -1(β) →LUMO+1(β) (17%)	$ILCT^{\theta}$
		243.92	0.0455	HOMO (α) →LUMO+1(α) (19%),	$ILCT^{\theta}$
				HOMO -7(β) →LUMO (β) (18%)	$LMCT^{\delta}$
		209.77	0.1642	HOMO -5(α) →LUMO (α) (21%)	$ILCT^{\theta}$
	B3PW91	502.42	0.0115	HOMO-10(β) →LUMO (β) (24%),	$LMCT^{\delta}$
				HOMO-7(β) →LUMO (β) (11%),	$LMCT^{\delta}$
				HOMO-6(β) →LUMO (β) (11%)	$LMCT^{\delta}$
		358.39	0.0567	HOMO (α) →LUMO (α) (34%),	$ILCT^{\theta}$
				HOMO (β) → LUMO +1(β) (37%)	$ILCT^{\theta}$
		311.53	0.1178	HOMO -2(β) →LUMO (β) (34%),	$LMCT^{\delta}$
				HOMO (β) → LUMO +2(β) (18%)	$ILCT^{\theta}$
		257.12	0.1884	HOMO -3(α) →LUMO (α) (21%),	$ILCT^{\theta}$
				HOMO -2(α) →LUMO (α) (12%),	$ILCT^{\theta}$
				HOMO -6 (β) →LUMO (β) (11%),	$LMCT^{\delta}$
				HOMO -4(β) →LUMO (β) (11%),	$LMCT^{\delta}$
				HOMO -1(β) → LUMO +1(β) (12%)	$ILCT^{\theta}$
		231.72	0.1854	HOMO (α) → LUMO +1(α) (26%),	$ILCT^{\theta}$
				HOMO (β) → LUMO +2(β) (37%)	$ILCT^{\theta}$
		204.17	0.0019	HOMO -1(α) → LUMO +3(α) (75%)	$LMCT^{\delta}$
	MPW1PW91	509.42	0.0073	HOMO-14(β) →LUMO (β) (10%),	$LMCT^{\delta}$
				HOMO-10(β) →LUMO (β) (32%),	$LMCT^{\delta}$
				HOMO-7(β) →LUMO (β) (12%)	$LMCT^{\delta}$
		346.49	0.0841	HOMO (α) → LUMO (α) (43%),	$ILCT^{\theta}$
				HOMO (β) → LUMO +1(β) (45%)	$ILCT^{\theta}$
		292.91	0.1766	HOMO -2(β) →LUMO (β) (69%)	$LMCT^{\delta}$
		255.69	0.2244	HOMO -2(α) →LUMO (α) (28%),	$ILCT^{\theta}$

				HOMO -1(β) → LUMO +1(β) (24%)	ILCT$^{\theta}$
		230.53	0.1228	HOMO (α) → LUMO +1(α) (17%),	ILCT$^{\theta}$
				HOMO (β) → LUMO +2(β) (34%)	ILCT$^{\theta}$
		202.24	0.0488	HOMO -1(α) → LUMO +3(α) (23%),	LMCT$^{\delta}$
				HOMO -6(β) →LUMO (β) (11%)	LMCT$^{\delta}$
2	B3LYP	512.77	0.0104	HOMO-11(β) →LUMO (β) (11%),	LMCT$^{\Gamma}$
				HOMO-9(β) →LUMO (β) (12%),	LMCT$^{\Gamma}$
				HOMO-4(β) →LUMO (β) (21%)	LMCT$^{\Gamma}$
		386.59	0.0592	HOMO (α) → LUMO (α) (42%),	ILCT$^{\Psi}$
				HOMO (β) →LUMO+1(β) (46%)	ILCT$^{\Psi}$
		320.46	0.1005	HOMO -2(β) → LUMO (β) (56%)	LMCT$^{\Gamma}$
		284.16	0.3282	HOMO -2(α) → LUMO (α) (32%),	ILCT$^{\Psi}$
				HOMO -2(β) →LUMO+1(β) (12%),	ILCT$^{\Psi}$
				HOMO -1(β) →LUMO+1(β) (34%)	ILCT$^{\Psi}$
		232.29	0.1648	HOMO (α) →LUMO +2(α) (28%),	ILCT$^{\Psi}$
				HOMO (β) →LUMO+3(β) (24%)	ILCT$^{\Psi}$
		206.87	0.0263	HOMO -2(α) →LUMO+1(α) (17%),	LMCT$^{\Gamma}$
				HOMO -1(β) →LUMO+2(β) (43%)	LMCT$^{\Gamma}$
	B3PW91	504.16	0.0111	HOMO-11(β) →LUMO (β) (10%),	LMCT$^{\Gamma}$
				HOMO-4(β) →LUMO (β) (20%)	LMCT$^{\Gamma}$
		382.36	0.0636	HOMO (α) →LUMO (α) (44%),	ILCT$^{\Psi}$
				HOMO(β) → LUMO +1(β) (46%)	ILCT$^{\Psi}$
		314.63	0.0985	HOMO -2(β) →LUMO (β) (56%)	LMCT$^{\Gamma}$
		279.61	0.2346	HOMO -2(α) →LUMO (α) (24%),	ILCT$^{\Psi}$
				HOMO -1(β) → LUMO +1(β) (28%)	ILCT$^{\Psi}$
		229.72	0.1110	HOMO(α) → LUMO +1(α) (17%),	ILCT$^{\Psi}$
				HOMO(β) → LUMO +2(β) (18%),	ILCT$^{\Psi}$
				HOMO(β) → LUMO +4(β)	LMCT$^{\Gamma}$
		203.52	0.0114	HOMO -1(α) → LUMO +3(α) (84%)	LMCT$^{\Gamma}$
	MPW1PW91	507.73	0.0073	HOMO-11(β) →LUMO (β) (16%)	LMCT$^{\Gamma}$
		367.79	0.0781	HOMO (α) →LUMO (α) (45%),	ILCT$^{\Psi}$
				HOMO (β) → LUMO +1(β) (48%)	ILCT$^{\Psi}$
		271.04	0.3710	HOMO -2(α) →LUMO (α) (30%),	ILCT$^{\Psi}$
				HOMO -2(β) → LUMO +1(β) (22%),	ILCT$^{\Psi}$
				HOMO -1(β) → LUMO +1(β) (30%)	ILCT$^{\Psi}$
		223.78	0.2144	HOMO (α) → LUMO +2(α) (33%),	LMCT$^{\Gamma}$
				HOMO (β) → LUMO +3(β) (31%)	LMCT$^{\Gamma}$
3	B3LYP	475.34	0.0082	HOMO-14(β) → LUMO (β) (15%),	LMCT$^{\Omega}$
				HOMO -13(β) →LUMO (β) 10%),	LMCT$^{\Omega}$
				HOMO -10(β) →LUMO (β) (25%)	LMCT$^{\Omega}$
		353.62	0.0247	HOMO-1(α) → LUMO (α) (70%)	ILCT$^{\Phi}$
		318.90	0.1882	HOMO-2(β) →LUMO (β) (60%)	LMCT$^{\Omega}$
		257.24	0.2603	HOMO-2(α) → LUMO (α) (22%),	ILCT$^{\Phi}$
				HOMO -4(β) →LUMO (β) (16%),	LMCT$^{\Omega}$
				HOMO -1(β) →LUMO+1(β) (20%)	ILCT$^{\Phi}$
		216.92	0.0126	HOMO-1(α) → LUMO+3(α) (55%)	LMCT$^{\Omega}$
	B3PW91	467.50	0.0077	HOMO-14(β) →LUMO (β) (11%),	LMCT$^{\Omega}$
				HOMO-13(β) →LUMO (β) (10%),	

				HOMO-10(β) →LUMO (β) (32%)	$LMCT^{\Omega}$
					$LMCT^{\Omega}$
		353.00	0.0534	HOMO -1(α) → LUMO (α) (36%)	$ILCT^{\Phi}$
		313.77	0.1583	HOMO -2(β) → LUMO (β) (55%)	$LMCT^{\Omega}$
		254.28	0.2614	HOMO -2(α) → LUMO (α) (21%),	$ILCT^{\Phi}$
				HOMO -4(β) → LUMO (β) (16%),	$LMCT^{\Omega}$
				HOMO -1(β) → LUMO +1(β) (18%)	$ILCT^{\Phi}$
		230.49	0.1704	HOMO(α) → LUMO +1(α) (21%),	$ILCT^{\Phi}$
				HOMO(β) → LUMO +2(β) (34%),	$ILCT^{\Phi}$
				HOMO(β) → LUMO +3(β) (12%)	$LMCT^{\Omega}$
		210.61	0.1818	HOMO (α) → LUMO +4(α) (20%),	$ILCT^{\Phi}$
				HOMO (β) → LUMO +5(β) (18%)	$ILCT^{\Phi}$
	MPW1PW91	475.01	0.0048	HOMO-14(β) → LUMO (β) (37%)	$LMCT^{\Omega}$
		344.50	0.0793	HOMO -1(α) → LUMO (α) (11%),	$ILCT^{\Phi}$
				HOMO (α) → LUMO (α)(37%),	$ILCT^{\Phi}$
				HOMO(β) → LUMO +1(β) (41%)	$ILCT^{\Phi}$
		296.01	0.1080	HOMO -2(β) → LUMO (β) (39%),	$LMCT^{\Omega}$
				HOMO -1(β) → LUMO (β) (25%)	$LMCT^{\Omega}$
		242.46	0.2061	HOMO -2(α) → LUMO (α) (10%),	$ILCT^{\Phi}$
				HOMO -4(β) → LUMO (β) (37%)	$LMCT^{\Omega}$
		206.23	0.0637	HOMO -8(β) → LUMO (β) (20%),	$LMCT^{\Lambda}$
				HOMO -5(β) → LUMO (β) (11%)	$LMCT^{\Omega}$

[g]$ILCT^{\theta}$ = intra ligand charge transfer transition in L^1; $ILCT^{\Psi}$= intra ligand charge transfer transition in L^2 ; $ILCT^{\Phi}$ = intra ligand charge transfer transition in L^3; $LMCT^{\delta}$= L^1 to metal charge transfer transition; $LMCT^{\Gamma}$= L^2 to metal charge transfer transition; $LMCT^{\Omega}$ = L^3 to metal charge transfer transition; $LMCT^{\Lambda}$ = water to metal charge transfer transition.

Table 7S. Comparative list of experimental and calculated[h] (using B3LYP, B3PW91, MPW1PW91functionals) electronic spectral bands of complexes **1-3**.

Complex	**Exp**	**Calcd**		
		B3LYP	B3PW91	MPW1PW91
1		512.03	502.42	509.42
	361	359.35	358.39	346.49
		318.10	311.53	292.91
	267	260.20	257.12	255.69
	241,249	243.92		
	224		231.72	230.53
	205	209.77	204.17	202.24

2		512.77	504.16	507.73
	375	386.59	382.36	367.79
		320.46	314.63	
	272	284.16	279.61	271.04
	236	232.29	229.72	223.78
	206	206.87	203.52	507.73
3		475.34	467.50	475.01
	355	353.62	353.00	344.50
		318.90	313.77	296.01
	266	257.24	254.28	242.46
	224		230.49	
	204	216.92	210.61	206.23

[h]Using conductor-like polarizable continuum model (CPCM) in methanol; basis set, LanL2DZ.

Table 8S. Selected UV-vis energy transition at the TD-DFT[i]/B3LYP level for HL^1, $HL^2$and HL^3 in methanol.

Schiff base	Excited state	λ_{cal} (nm), ε_{cal} ($M^{-1}cm^{-1}$), (eV)	Oscillator strength (f)	λ_{exp} (nm), ε_{exp} ($M^{-1}cm^{-1}$), (eV)	Key transition	Character
HL^1	S_3	279.62, 11751, (4.434)	0.1582	279, 4.5 x 10^4, (4.443)	HOMO -1 → LUMO (83%)	π → π*
	S_4	253.72, 6644, (4.886)	0.0066	255, 13.57 x 10^4, (4.862)	HOMO -2 → LUMO (98%)	n → π*
HL^2	S_2	296.12, 5647, (4.186)	0.0011	296, 5.04 x 10^4, (4.188)	HOMO-1 → LUMO (99%)	n → π*
	S_6	217.54, 34706, (5.699)	0.0055	220, 19.06 x 10^4, (5.635)	HOMO-1 → LUMO+1 (96%)	n → π*
	S_8	207.03, 28186, (5.988)	0.0964	207, 17.51 x 10^4, (5.989)	HOMO-2 → LUMO+1 (65%)	π → π*
HL^3	S_2	275.58, 10552, (4.499)	0.0816	275, 6.69 x 10^4,(4.508)	HOMO-1→LUMO (33%)	π → π*
	S_9	202.52, 19318, (6.122)	0.0602	206, 27.81 x 10^4,(6.018)	HOMO → LUMO+2 (79%)	n → π*

[i] Using conductor-like polarizable continuum model (CPCM) in methanol; basis set,6-31G(d-p).

Table 9S. Calculated (using B3LYP functional) list of excitation energies of HL^1. [Using conductor-like polarizable continuum model (CPCM) in methanol; basis set, 6-31 G (d-p)].

Excitation	Wavelength λ (nm)	Oscillatory strength (*f*)	Major Contribution	Assignment
1	299.52	0.0006	HOMO→LUMO (98%)	n→ π*
2	281.40	0.0038	HOMO -4→LUMO (40%), HOMO -3→LUMO (55%)	π→π* π→π*
3	279.62	0.1582	HOMO -1→LUMO (83%)	π→π*
4	253.72	0.0066	HOMO -2→LUMO (98%)	n→π*
5	239.83	0.4102	HOMO -4→LUMO (43%), HOMO -1→LUMO (12%), HOMO -1→LUMO+1 (16%)	π→π* π→π* π→π*
6	225.81	0.0021	HOMO→LUMO+1 (99%)	n→π*
7	209.42	0.3741	HOMO -1→LUMO+1 (65%)	π→π*
8	205.87	0.0029	HOMO -4→LUMO+1 (38%), HOMO -3→LUMO+1 (59%)	π→π* π→π*
9	201.69	0.0117	HOMO -2→LUMO+1 (98%)	n→π*
10	194.35	0.3285	HOMO -4→LUMO+1 (45%), HOMO -1→LUMO+2 (12%)	π→π* π→π*
11	185.94	0.0067	HOMO→LUMO+2 (79%)	n→π*
12	184.12	0.0218	HOMO -5→LUMO (51%), HOMO →LUMO+2 (19%)	π→π* n→π*
13	177.65	0.0023	HOMO -7→LUMO (31%),	n→π*
14	175.10	0.1017	HOMO -1→LUMO+2 (30%)	π→π*
15	174.47	0.0718	HOMO -7→LUMO (14%), HOMO -3→LUMO+2 (32%), HOMO -1→LUMO+2 (19%)	n→π* π→π* π→π*
18	167.36	0.0028	HOMO -2→LUMO+2 (93%)	n→π*
20	165.94	0.0119	HOMO -11→LUMO (23%), HOMO -10→LUMO (25%), HOMO -8→LUMO (18%), HOMO -7→LUMO (12%)	π→π* π→π* π→π* n→π*
21	165.23	0.0099	HOMO -11→LUMO (25%), HOMO -10→LUMO (18%)	π→π* π→π*
22	162.77	0.0187	HOMO -8→LUMO (35%)	π→π*
24	160.97	0.0473	HOMO -10→LUMO (22%)	π→π*
25	160.69	0.0157	HOMO→LUMO+5 (15%)	n→π*
26	159.56	0.0064	HOMO -9→LUMO (28%)	n→π*
27	158.92	0.0002	HOMO -1→LUMO+5 (79%)	π→π*
28	155.87	0.0755	HOMO -5→LUMO+1 (32%)	π→π*
31	154.90	0.0424	HOMO -12→LUMO (16%), HOMO -9→LUMO (30%)	n→π* n→π*
32	153.13	0.0008	HOMO -7→LUMO+1 (26%)	n→π*
34	151.52	0.0029	HOMO→LUMO+5 (54%)	n→π*
36	150.62	0.0044	HOMO -12→LUMO (34%)	n→π*
40	147.46	0.0017	HOMO -4→LUMO+5 (42%)	π→π*
43	145.14	0.0015	HOMO -11→LUMO+1 (29%)	π→π*
45	144.21	0.0043	HOMO -13→LUMO (35%), HOMO -11→LUMO+1	π→π* π→π*

			(34%)	
47	142.78	0.0097	HOMO -2→LUMO+5 (14%)	n→π*
48	142.65	0.0923	HOMO -8→LUMO+1 (25%),	π→π*
			HOMO -4→LUMO+5 (13%),	π→π*
			HOMO -3→LUMO+5 (18%)	π→π*
49	141.58	0.0656	HOMO -8→LUMO+1 (16%)	π→π*
50	141.00	0.0094	HOMO -2→LUMO+5 (30%)	n→π*

Table 10S. Calculated (using B3LYP functional) list of excitation energies of HL^2. [Using conductor-like polarizable continuum model (CPCM) in methanol; basis set, 6-31 G (d-p)].

Excitation	Wavelength λ (nm)	Oscillatory strength (*f*)	Major Contribution	Assignment
1	299.16	0.0791	HOMO→LUMO (93%)	π→π*
2	296.12	0.0011	HOMO-1→LUMO (99%)	n→π*
3	279.49	0.0019	HOMO-4→LUMO (97%)	π→π*
4	251.48	0.0761	HOMO-3→LUMO (60%)	n→π*
5	246.73	0.4164	HOMO-3→LUMO (38%),	n→π*
			HOMO-2→LUMO (55%)	π→π*
6	217.54	0.0055	HOMO-1→LUMO+1 (96%)	n→π*
7	213.56	0.5707	HOMO→LUMO+1 (87%)	π→π*
8	207.03	0.0964	HOMO-2→LUMO+1 (65%)	π→π*
10	195.15	0.0001	HOMO-3→LUMO+1 (91%)	n→π*
11	191.09	0.0516	HOMO-5→LUMO (75%)	π→π*
12	182.61	0.0034	HOMO-1→LUMO+2 (98%)	n→π*
13	182.27	0.0003	HOMO→LUMO+3 (98%)	π→π*
14	180.22	0.3551	HOMO-5→LUMO (10%),	π→π*
			HOMO-2→LUMO+1 (18%),	π→π*
			HOMO→LUMO+2 (54%)	π→π*
15	175.30	0.0028	HOMO-8→LUMO (12%),	n→π*
			HOMO-4→LUMO+2 (38%)	π→π*
17	172.77	0.0006	HOMO-7→LUMO (26%),	n→π*
			HOMO-4→LUMO+2 (57%)	π→π*
18	170.50	0.0362	HOMO-6→LUMO (41%)	n→π*
19	168.10	0.0002	HOMO-9→LUMO (79%),	n→π*
			HOMO-8→LUMO (12%)	n→π*
20	166.09	0.0168	HOMO-1→LUMO+5 (12%)	n→π*
21	165.66	0.0217	HOMO-6→LUMO (37%),	n→π*
			HOMO-2→LUMO+2 (28%)	π→π*
22	164.62	0.0070	HOMO-3→LUMO+2 (76%)	n→π*
23	164.48	0.0002	HOMO-2→LUMO+3 (58%)	π→π*
24	163.12	0.0011	HOMO-2→LUMO+3 (25%),	π→π*
			HOMO-1→LUMO+3 (67%)	n→π*
25	162.68	0.0012	HOMO→LUMO+5 (72%)	π→π*
26	161.93	0.0258	HOMO-10→LUMO (17%),	n→π*
			HOMO-8→LUMO (36%),	n→π*
			HOMO-7→LUMO (23%)	n→π*
28	160.88	0.0665	HOMO-12→LUMO (17%),	n→π*
			HOMO-10→LUMO (48%)	n→π*
30	159.06	0.0585	HOMO-12→LUMO (36%),	n→π*
			HOMO-8→LUMO (10%),	n→π*

			HOMO-5→LUMO+1 (28%)	π→π*
31	157.57	0.0730	HOMO-11→LUMO (22%),	n→π*
			HOMO-10→LUMO (13%),	n→π*
			HOMO-5→LUMO+1 (38%)	π→π*
32	155.20	0.0067	HOMO-13→LUMO (26%),	n→π*
			HOMO-11→LUMO (42%)	n→π*
35	151.70	0.0009	HOMO-4→LUMO+3 (93%)	π→π*
36	151.21	0.0011	HOMO-2→LUMO+5 (41%)	π→π*
38	150.56	0.0001	HOMO-3→LUMO+3 (86%)	n→π*
39	150.33	0.0021	HOMO-1→LUMO+5 (18%)	n→π*
40	150.24	0.0009	HOMO-14→LUMO (21%),	π→π*
			HOMO-13→LUMO (15%),	n→π*
			HOMO-1→LUMO+5 (16%)	n→π*
41	149.50	0.0011	HOMO-2→LUMO+5 (29%)	π→π*
42	148.84	0.0004	HOMO-7→LUMO+1 (45%)	n→π*
44	147.95	0.0050	HOMO-14→LUMO (39%)	π→π*
49	144.62	0.0001	HOMO-12→LUMO+1 (15%),	n→π*
			HOMO-9→LUMO+1 (59%)	n→π*

Table 11S. Calculated (using B3LYP functional) list of excitation energies of HL^3. [Using conductor-like polarizable continuum model (CPCM) in methanol; basis set, 6-31 G (d-p)].

Excitation	**Wavelength λ (nm)**	**Oscillatory strength (*f*)**	**Major Contribution**	**Assignment**
1	279.82	0.0343	HOMO→LUMO (71%)	n→π*
2	275.58	0.0816	HOMO-1→LUMO (33%)	π→π*
3	267.98	0.0454	HOMO-3→LUMO (25%),	π→π*
			HOMO-1→LUMO (55%)	π→π*
4	236.39	0.0459	HOMO-2→LUMO (61%)	n→π*
5	232.93	0.1127	HOMO-4→LUMO (54%),	π→π*
			HOMO-1→LUMO+1 (17%)	π→π*
6	224.39	0.0126	HOMO→LUMO+1 (85%)	n→π*
7	214.12	0.1193	HOMO-1→LUMO+1 (26%)	π→π*
8	211.12	0.0712	HOMO-3→LUMO+1 (34%),	π→π*
			HOMO-2→LUMO+1 (27%)	n→π*
9	202.51	0.0602	HOMO→LUMO+2 (79%)	n→π*
10	198.52	0.0391	HOMO-2→LUMO+1 (43%),	n→π*
			HOMO-1→LUMO+2 (13%)	π→π*
11	198.42	0.1747	HOMO-3→LUMO+1 (13%),	π→π*
			HOMO-1→LUMO+1 (14%),	π→π*
			HOMO-1→LUMO+2 (23%)	π→π*
12	195.20	0.0150	HOMO-3→LUMO+2 (54%),	π→π*
			HOMO-2→LUMO+2 (24%)	n→π*
13	191.75	0.1247	HOMO-5→LUMO (59%),	π→π*
			HOMO-4→LUMO+1 (11%),	π→π*
			HOMO-4→LUMO+2 (17%)	π→π*
14	185.21	0.2146	HOMO-5→LUMO+1 (13%),	π→π*
			HOMO-4→LUMO+1 (41%),	π→π*
			HOMO-1→LUMO+2 (29%)	π→π*

15	178.56	0.0013	HOMO-2→LUMO+2 (65%)	n→π*
17	172.32	0.0228	HOMO-6→LUMO (57%)	n→π*
19	170.60	0.0637	HOMO-6→LUMO (10%),	n→π*
			HOMO-4→LUMO+2 (36%)	π→π*
20	167.33	0.2054	HOMO-5→LUMO+1 (63%)	π→π*
21	167.30	0.0569	HOMO→LUMO+6 (13%)	n→π*
22	162.27	0.0082	HOMO-1→LUMO+6 (12%)	π→π*
25	160.28	0.1348	HOMO-7→LUMO (73%)	π→π*
26	159.37	0.0013	HOMO-9→LUMO (39%)	n→π*
27	157.64	0.0054	HOMO-11→LUMO (42%),	π→π*
			HOMO-8→LUMO (35%),	n→π*
			HOMO-6→LUMO (10%)	n→π*
28	156.62	0.0028	HOMO-1→LUMO+6 (18%)	π→π*
30	155.35	0.0019	HOMO-10→LUMO (25%),	n→π*
			HOMO-8→LUMO (35%)	n→π*
32	153.95	0.0046	HOMO-6→LUMO+1 (20%),	n→π*
			HOMO→LUMO+6 (13%)	n→π*
33	153.90	0.0294	HOMO-6→LUMO+1 (23%)	n→π*
34	153.40	0.0324	HOMO-10→LUMO (23%),	n→π*
			HOMO-9→LUMO (15%)	n→π*
35	152.89	0.0045	HOMO-1→LUMO+6 (25%)	π→π*
38	150.34	0.1644	HOMO-10→LUMO (11%),	n→π*
			HOMO-5→LUMO+2 (57%)	π→π*
39	149.94	0.0035	HOMO→LUMO+6 (13%)	n→π*
44	146.86	0.0118	HOMO-13→LUMO (11%),	n→π*
			HOMO-12→LUMO (55%)	n→π*
45	144.73	0.0307	HOMO-11→LUMO+1 (21%),	π→π*
			HOMO-7→LUMO+1 (55%)	π→π*
46	144.45	0.0088	HOMO-4→LUMO+6 (15%)	π→π*
47	143.58	0.0206	HOMO-3→LUMO+6 (33%),	π→π*
			HOMO-2→LUMO+6 (36%)	n→π*
48	143.30	0.0040	HOMO-11→LUMO+1 (23%)	π→π*
49	143.20	0.0258	HOMO-11→LUMO+1 (35%)	π→π*

Table 12S. List of selected excitation bands of HL^1, $HL^2$and HL^3calculated in different functionals (B3LYP, B3PW91, MPW1PW91) in CPCM model in methanolic solution. [Basis set, 6-31G (d-p)].

Schiff base	**Functional**	**Wavelength λ (nm)**	**Oscillatory strength (*f*)**	**Major Contribution**	**Assignment**
HL^1	B3LYP	279.62	0.1582	HOMO -1→LUMO (83%)	π→π*
		239.83	0.4102	HOMO-4→LUMO (43%),	π→π*
				HOMO-1→LUMO (12%),	π→π*

				HOMO-1→LUMO+1 (16%)	π→π*
		209.42	0.3741	HOMO-1→LUMO+1 (65%)	π→π*
	B3PW91	278.56	0.1652	HOMO-1→LUMO (84%)	π→π*
		238.25	0.4166	HOMO-4→LUMO (68%)	π→π*
		208.60	0.3597	HOMO-4→LUMO (18%),	π→π*
				HOMO-1→LUMO+1 (63%)	π→π*
	MPW1PW91	271.73	0.1782	HOMO-1→LUMO (85%)	π→π*
		233.91	0.3617	HOMO-3→LUMO (55%)	π→π*
		203.81	0.4432	HOMO-3→LUMO (18%),	π→π*
				HOMO-1→LUMO+1 (68%)	π→π*
HL^2	B3LYP	299.16	0.0791	HOMO→LUMO (93%)	π→π*
		246.73	0.4164	HOMO-3→LUMO (38%),	n→π*
				HOMO-2→LUMO (55%)	π→π*
		213.56	0.5707	HOMO→LUMO+1 (87%)	π→π*
	B3PW91	298.704	0.0794	HOMO→LUMO (82%)	π→π*
		246.06	0.4736	HOMO-3→LUMO (52%)	n→π*
		213.05	0.5670	HOMO→LUMO+1 (83%)	π→π*
	MPW1PW91	289.27	0.0895	HOMO→LUMO (93%)	π→π*
		241.78	0.4620	HOMO-2→LUMO (93%)	π→π*
		208.93	0.6182	HOMO→LUMO+1 (90%)	π→π*
HL^3	B3LYP	275.58	0.0816	HOMO-1→LUMO (33%)	π→π*

	232.93	0.1127	HOMO-4→LUMO (54%),	π→π*
			HOMO-1→LUMO+1 (17%)	π→π*
	214.12	0.1193	HOMO-1→LUMO+1 (26%)	π→π*
B3PW91	275.48	0.0531	HOMO-3→LUMO (44%),	n→π*
			HOMO-2→LUMO (13%)	n→π*
	231.77	0.1334	HOMO-4→LUMO (52%),	π→π*
			HOMO-1→LUMO+1 (19%)	π→π*
	210.99	0.1156	HOMO-3→LUMO+1 (27%),	n→π*
			HOMO-2→LUMO+1 (15%),	n→π*
			HOMO-1→LUMO+1 (16%)	π→π*
MPWIPW91	265.53	0.1541	HOMO→LUMO (58%)	n→π*
	227.74	0.1580	HOMO-4→LUMO (49%),	π→π*
			HOMO-1→LUMO+1 (22%)	π→π*
	206.64	0.1834	HOMO-1→LUMO+1 (36%)	π→π*

Table 13S. Comparative list of experimental and calculated[j] (using B3LYP, B3PW91, MPW1PW91functionals) electronic spectral bands of HL^1, HL^2 and HL^3.

Ligand	**Exp**	**Calcd**		
		B3LYP	**B3PW91**	**MPW1PW91**
HL^1	400			
	316			
	279	279.62	278.56	271.73
	255	239.83	238.25	233.91
	215	209.42	208.60	203.81
HL^2	422			
	296	299.16	298.704	289.27
	220, 263	246.73	246.06	241.78

	207	213.56	213.05	208.93
HL^3	389			
	316			
	275	275.58	275.48	265.53
		232.93	231.77	227.74
	206	214.12	210.99	206.64

[j]Basis set, 6-31G (d-p); using conductor-like polarizable continuum model (CPCM) in methanol.

Table 14S. Selected experimental[k] and calculated [l] IR bands (cm^{-1}) and their assignments for complexes **1**, **2** and **3**.

	Complex 1		**Complex 2**		**Complex 3**	
	Exp	**Calcd**	**exp**	**calcd**	**exp**	**calcd**
ν(O-H) stretching (H-bonded)	3200-3500 (br,vs)	3477(w), 3235(w), 3221(w)	3200-3500 (br,vs)	3478(w), 3240(w), 3221(w), 3190(w)	3200-3500 (br,vs)	3477(w), 3251(w), 3227(w), 3215(w)
ν_s(C-O) stretching	1300(s)	1324(s),1269(w), 1242(s)	1297(s)	1252(vs),1215(w), 1196(w)	1300(s)	1268(s)
ν(C-H) stretching (aromatic rings)	2972(s)	3073(w),3049(w),	2975(s)	3072(w),3039(w),3045(w)	2982(s)	3069(w),3046(w)
ν(C-H) stretching (SP^3 hybridized)	2943(s)	-	2943(s)	-	2943(s)	-
ν(N-H) stretching (SP^3 hybridized)	3102(s)	3143(w),3113(w)	-	3126(w),3112(w)	3094(s)	3139(w),3129(w), 3125(w)
$\nu(C=C)_{aromatic}$	1649(s),1561(vs)	1657(vs),1644(w), 1627(w), 1566(s),	1639(vs),1558(vs)	1656(vs),1640(s),1620(s)	1643(vs),1561(vs)	1644(s),1618(vs), 1614(vs),1567(s)
$\nu(C=N)_{aromatic}$	1460(s),1418(s), 1372(s)	1469(w),1439(w), 1398(w),	1467(s),1418(vs), 1372(s)	1461(s),1439(s)	1467(vs),1414(vs),1372(s)	1541(w),1504(w), 1496(w), 1457(s)
$\nu(ClO_4)$	1115(s),1072(s)	1115(w)	1124(w),1079(s)	1122(w), 1114(w), 1098(w)	1124(s),1108(s), 1082(s)	1115(w),1106(w), 1097(w)
$\rho_w(H_2O)$	515(s)	536(w)	515(s)	546(w)	551(s)	536(w)

[k] In solid state as KBr pellet. [l] Basis set LanL2DZ; B3LYP functional. vs = very strong, s = strong, w = weak, br = broad.

Table 15S. Calculated energies of optimized geometries and other physical parameters for complexes **1**, **2** and **3**, using B3LYP, B3PW91 and MPW1PW91 functionals. (In methanol using CPCM model, basis set LanL2DZ).

Complex	Parameters	Functional		
		B3LYP	**B3PW91**	**MPW1PW91**
1	Energy (eV)	-25598.342	-25591.952	-25593.978
	Dipole Moment	11.8159	11.7622	11.8396
	Point Group	C1	C1	C1
2	Energy (eV)	-28714.196	-28706.606	-28709.021
	Dipole Moment	11.7993	11.7850	11.7990
	Point Group	C1	C1	
3	Energy (eV)	-26667.913	-26661.184	-26663.357
	Dipole Moment	11.8009	11.7330	11.8177
	Point Group	C1	C1	C1

Table 16S. Selected MOs along with their energy and compositions of **1**.

MOs	Energy (eV)	% of Composition		
		L[1]	**Aqua**	**Cu**
α-Mos				
LUMO+15	3.99	59	40	1
LUMO+14	3.72	74	9	17
LUMO+13	3.6	96	1	3
LUMO+12	3.52	88	3	9
LUMO+11	3.43	79	20	1
LUMO+10	2.95	92	0	8
LUMO+9	2.82	89	3	8
LUMO+8	2.63	70	14	16
LUMO+7	2.53	90	8	2
LUMO+6	0.86	11	5	84
LUMO+5	0.6	72	1	27
LUMO+4	0.47	16	1	83
LUMO+3	0.08	15	1	84
LUMO+2	-0.1	41	13	46
LUMO+1	-0.27	59	6	35
LUMO	-1.96	99	0	1

HOMO	-5.97	97	0	3
HOMO -1	-6.53	81	0	19
HOMO -2	-7.13	99	0	1
HOMO -3	-7.87	92	1	7
HOMO -4	-8.4	46	16	38
HOMO -5	-8.8	72	7	21
HOMO -6	-8.94	89	0	11
HOMO -7	-9.21	65	15	20
HOMO -8	-9.41	41	54	5
HOMO -9	-9.81	60	12	28
HOMO -10	-9.94	72	0	28
HOMO -11	-10.05	36	1	63
HOMO -12	-10.06	37	3	60
HOMO -13	-10.27	83	1	16
HOMO -14	-10.41	91	2	7
HOMO -15	-10.54	31	0	69
β-MOs				
LUMO+15	3.73	73	10	17
LUMO+14	3.62	95	1	4
LUMO+13	3.53	89	2	9
LUMO+12	3.45	78	21	1
LUMO+11	2.96	92	0	8
LUMO+10	2.83	90	3	7
LUMO+9	2.65	72	12	16
LUMO+8	2.56	86	10	4
LUMO+7	0.89	11	6	83
LUMO+6	0.61	72	1	27
LUMO+5	0.47	17	1	82
LUMO+4	0.09	14	1	85
LUMO+3	-0.1	41	13	46
LUMO+2	-0.26	59	6	35
LUMO+1	-1.92	99	0	1
LUMO	-2.75	40	0	60
HOMO	-5.92	97	0	3
HOMO -1	-7.09	98	0	2
HOMO -2	-7.42	92	1	7
HOMO -3	-7.98	37	11	52
HOMO -4	-8.46	71	3	26
HOMO -5	-8.79	80	1	19
HOMO -6	-8.85	50	9	41
HOMO -7	-9.16	73	1	26
HOMO -8	-9.4	16	60	24
HOMO -9	-9.66	38	11	51
HOMO -10	-9.75	54	0	46
HOMO -11	-9.77	49	10	41
HOMO -12	-10.02	92	0	8
HOMO -13	-10.27	71	1	28
HOMO -14	-10.34	56	1	43
HOMO -15	-10.39	89	2	9

Table 17S. Selected MOs along with their energies and compositions of **2**.

MOs	Energy (eV)	% of composition		
		L^2	Aqua	Cu
α-MOs				
LUMO+15	3.61	90	3	7
LUMO+14	3.53	97	1	2
LUMO+13	3.44	76	21	3
LUMO+12	3.4	90	1	9
LUMO+11	2.98	92	0	8
LUMO+10	2.82	88	4	8
LUMO+9	2.64	70	14	16
LUMO+8	2.54	96	4	0
LUMO+7	2.13	95	4	1
LUMO+6	0.86	24	4	72
LUMO+5	0.66	70	1	29
LUMO+4	0.45	8	1	91
LUMO+3	0.08	20	1	79
LUMO+2	-0.01	85	2	13
LUMO+1	-0.18	11	17	72
LUMO	-1.92	99	0	1
HOMO	-5.68	98	0	2
HOMO -1	-6.54	82	0	18
HOMO -2	-6.75	98	0	2
HOMO -3	-7.86	92	1	7
HOMO -4	-8.41	48	15	37
HOMO -5	-8.6	91	1	8
HOMO -6	-8.82	78	6	16
HOMO -7	-9.0	82	0	18
HOMO -8	-9.01	97	2	1
HOMO -9	-9.37	27	63	10
HOMO -10	-9.56	77	8	15
HOMO -11	-9.92	52	8	40
HOMO -12	-10.07	41	0	59
HOMO -13	-10.11	31	4	65
HOMO -14	-10.2	67	0	33
HOMO -15	-10.41	90	3	7
β-MOs				
LUMO+15	3.54	97	1	2
LUMO+14	3.45	76	22	2
LUMO+13	3.40	91	1	8
LUMO+12	2.99	92	0	8
LUMO+11	2.84	89	3	8
LUMO+10	2.65	70	13	17
LUMO+9	2.57	93	6	1
LUMO+8	2.14	95	4	1
LUMO+7	0.9	20	5	75
LUMO+6	0.67	75	1	24
LUMO+5	0.45	9	1	90
LUMO+4	0.9	19	1	80
LUMO+3	-0.0	85	2	13
LUMO+2	-0.18	12	17	71
LUMO+1	-1.88	99	0	1
LUMO	-2.76	40	0	60
HOMO	-5.64	98	0	2

HOMO -1	-6.71	97	0	3
HOMO -2	-7.43	92	1	7
HOMO -3	-7.99	37	11	52
HOMO -4	-8.45	73	2	25
HOMO -5	-8.55	86	2	12
HOMO -6	-8.82	70	0	30
HOMO -7	-8.91	75	8	17
HOMO -8	-9.06	88	3	9
HOMO -9	-9.38	47	9	44
HOMO -10	-9.41	25	54	21
HOMO -11	-9.77	46	9	45
HOMO -12	-9.81	63	5	32
HOMO -13	-9.85	47	3	50
HOMO -14	-10.25	50	0	50
HOMO -15	-10.37	91	3	6

Table 18S. Selected MOs along with their energies and compositions of **3**.

MOs	**Energy (eV)**	**(%) of composition**		
		L^3	**Aqua**	**Cu**
α-MOs				
LUMO+15	3.77	82	12	6
LUMO+14	3.73	79	7	14
LUMO+13	3.64	90	1	9
LUMO+12	3.5	85	14	1
LUMO+11	3.21	91	5	4
LUMO+10	2.97	95	1	4
LUMO+9	2.91	88	2	10
LUMO+8	2.58	89	6	5
LUMO+7	2.56	68	19	13
LUMO+6	0.8	23	4	73
LUMO+5	0.56	66	1	33
LUMO+4	0.47	14	0	86
LUMO+3	0.08	17	1	82
LUMO+2	-0.04	63	8	29
LUMO+1	-0.2	34	11	55
LUMO	-1.85	99	0	1
HOMO	-5.9	97	0	3
HOMO -1	-6.45	81	0	19
HOMO -2	-7.08	99	0	1
HOMO -3	-7.83	93	1	6
HOMO -4	-8.35	44	17	39
HOMO -5	-8.63	81	2	17
HOMO -6	-8.87	87	0	13
HOMO -7	-8.93	82	7	11
HOMO -8	-9.34	31	62	7
HOMO -9	-9.73	62	14	24
HOMO -10	-9.85	72	1	27
HOMO -11	-9.96	31	0	69
HOMO -12	-9.98	31	3	66
HOMO -13	-10.19	82	2	16
HOMO -14	-10.36	93	1	6
HOMO -15	-10.48	34	1	65
β-MOs				
LUMO+15	3.73	79	8	13

LUMO+14	3.65	89	1	10
LUMO+13	3.51	86	13	1
LUMO+12	3.23	91	5	4
LUMO+11	2.99	94	1	5
LUMO+10	2.92	88	2	10
LUMO+9	2.61	99	1	0
LUMO+8	2.57	58	23	19
LUMO+7	0.84	20	5	75
LUMO+6	0.57	68	1	31
LUMO+5	0.47	15	0	85
LUMO+4	0.09	16	1	83
LUMO+3	-0.02	64	8	28
LUMO+2	-0.2	35	10	55
LUMO+1	-1.8	97	0	3
LUMO	-2.67	42	0	58
HOMO	-5.85	97	0	3
HOMO -1	-7.04	98	0	2
HOMO -2	-7.38	93	1	6
HOMO -3	-7.94	35	12	53
HOMO -4	-8.33	78	1	21
HOMO -5	-8.71	63	2	35
HOMO -6	-8.75	81	4	15
HOMO -7	-8.98	79	4	17
HOMO -8	-9.35	18	55	27
HOMO -9	-9.53	30	8	62
HOMO -10	-9.63	50	2	48
HOMO -11	-9.68	38	16	46
HOMO -12	-9.9	95	0	5
HOMO -13	-10.16	61	0	39
HOMO -14	-10.3	67	1	32
HOMO -15	-10.36	87	1	12

Table 19S. Calculated energies of optimized geometries and other physical parameters for **HL[1]**, **HL[2]** and **HL[3]**, using B3LYP, B3PW91 and MPW1PW91 functionals.(In methanol, using CPCM model, basis set 6-31G (d-p).

Ligand	**Parameters**	**Functional**		
		B3LYP	**B3PW91**	**MPW1PW91**
HL^1	Energy	-18201.337	-18194.514	-18197.028
	Dipole Moment	1.3558	1.3672	1.3892
	Point Group	C1	C1	C1
HL^2	Energy	-21317.768	-21309.761	-21312.693

	Dipole Moment	2.6115	2.5677	2.5720
	Point Group	C1	C1	C1
HL^3	Energy	-19271.103	-19263.924	-19266.585
	Dipole Moment	0.9708	1.0517	1.0376
	Point Group	C1	C1	C1

Table 20S. Selected MOs along with their energies and compositions of **HL^1**.

MOs	**Energy (eV)**	**% of Composition**			
		Benzene ring	**Phenolic–OH**	**C=N bond**	**Rest part**
LUMO+10	4.18	23	0	1	76
LUMO+9	3.71	19	1	7	73
LUMO+8	3.41	13	0	13	74
LUMO+7	3.11	12	0	14	74
LUMO+6	2.77	20	1	7	72
LUMO+5	2.68	70	2	13	15
LUMO+4	2.3	0	1	1	98
LUMO+3	2.25	23	76	0	1
LUMO+2	1.4	54	0	43	3
LUMO+1	0.08	94	4	2	0
LUMO	-1.12	56	2	39	3
HOMO	-5.89	1	0	1	98
HOMO-1	-6.11	69	17	10	4
HOMO-2	-6.5	2	0	0	98
HOMO-3	-6.74	34	2	54	10
HOMO-4	-6.76	48	2	41	9
HOMO-5	-8.46	34	0	38	28
HOMO-6	-9.2	13	3	4	80
HOMO-7	-9.23	37	9	8	46
HOMO-8	-9.36	47	25	4	24
HOMO-9	-9.63	7	3	8	82
HOMO-10	-9.7	45	7	9	39

Table 21S. Selected MOs along with their energies and compositions of **HL^2**.

MOs	Energy (eV)	% of Composition				
		Benzene ring	Phenolic -OH	C=N bond	-OMe	Rest part
LUMO+10	3.8	20	17	9	12	42
LUMO+9	3.53	9	7	5	9	70
LUMO+8	3.34	21	2	4	19	54
LUMO+7	3.09	10	0	15	19	56
LUMO+6	2.81	12	3	3	20	62
LUMO+5	2.7	35	2	16	22	25
LUMO+4	2.3	0	0	1	0	99
LUMO+3	2.11	45	32	2	21	0
LUMO+2	1.5	53	0	43	1	3
LUMO+1	0.26	93	3	0	4	0
LUMO	-1.07	51	3	42	1	3
HOMO	-5.79	68	15	2	14	1
HOMO-1	-5.9	1	0	0	0	99
HOMO-2	-6.39	61	2	18	6	13
HOMO-3	-6.52	7	0	1	1	91
HOMO-4	-6.76	4	2	80	0	14
HOMO-5	-8.19	30	1	34	16	19
HOMO-6	-9.08	33	3	4	20	40
HOMO-7	-9.21	21	3	6	9	61
HOMO-8	-9.29	24	3	7	20	46
HOMO-9	-9.4	23	7	5	37	28
HOMO-10	-9.47	36	37	0	27	0

Table 22S. Selected MOs along with their energies and compositions of **HL^3**.

MOs	Energy (eV)	% of Composition				
		Benzene ring	Pheolic–OH	C=N bond	$-CH_3$	Rest part
LUMO+10	3.81	21	1	1	26	51
LUMO+9	3.8	12	0	2	30	56
LUMO+8	3.2	0	0	1	7	92
LUMO+7	3.17	13	1	1	22	63
LUMO+6	2.81	58	3	2	1	36
LUMO+5	2.5	24	1	3	26	46
LUMO+4	2.3	24	75	0	0	1
LUMO+3	2.28	1	1	1	4	93
LUMO+2	0.88	51	1	39	5	4
LUMO+1	0.14	90	4	4	2	0
LUMO	-0.79	57	1	36	3	3
HOMO	-5.83	6	1	2	0	91
HOMO-1	-6.05	69	18	5	0	8
HOMO-2	-6.46	2	0	19	3	76
HOMO-3	-6.57	6	1	51	7	35
HOMO-4	-6.73	78	1	13	1	7
HOMO-5	-7.92	25	1	51	8	15
HOMO-6	-9.02	26	5	9	2	58
HOMO-7	-9.18	66	29	2	2	1
HOMO-8	-9.22	8	2	3	1	86
HOMO-9	-9.49	30	10	5	1	54
HOMO-10	-9.59	5	1	4	6	84

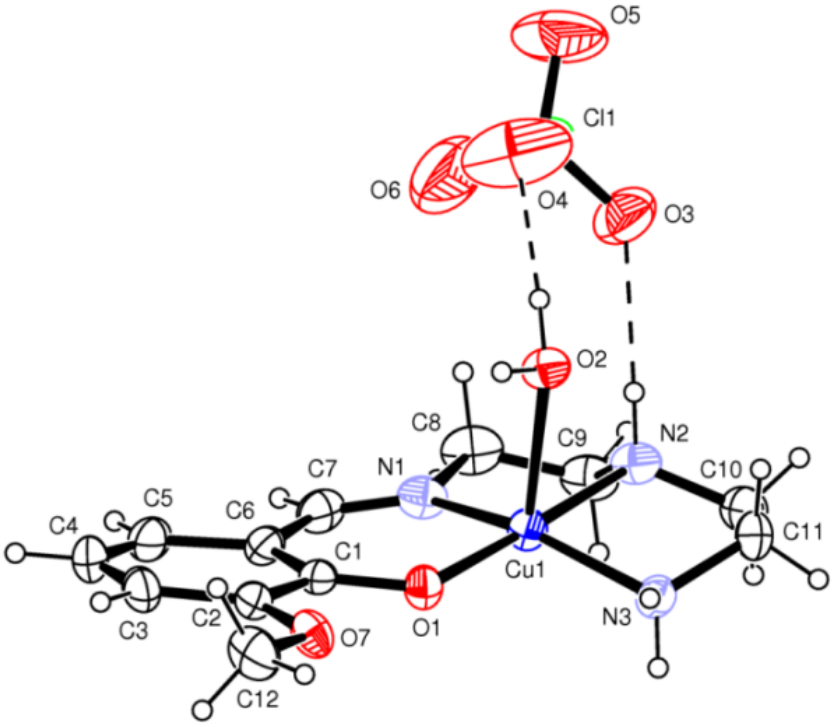

Fig.1S. ORTEP diagram (ellipsoids at 30% probability) of **2**.

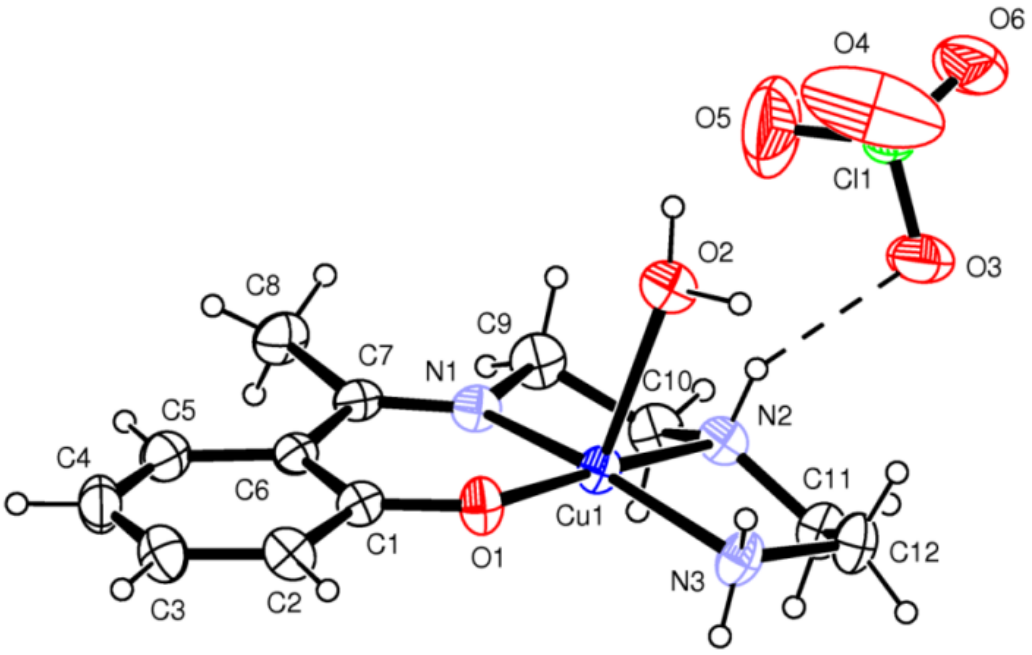

Fig. 2S. ORTEP diagram (ellipsoids at 30% probability) of **3**.

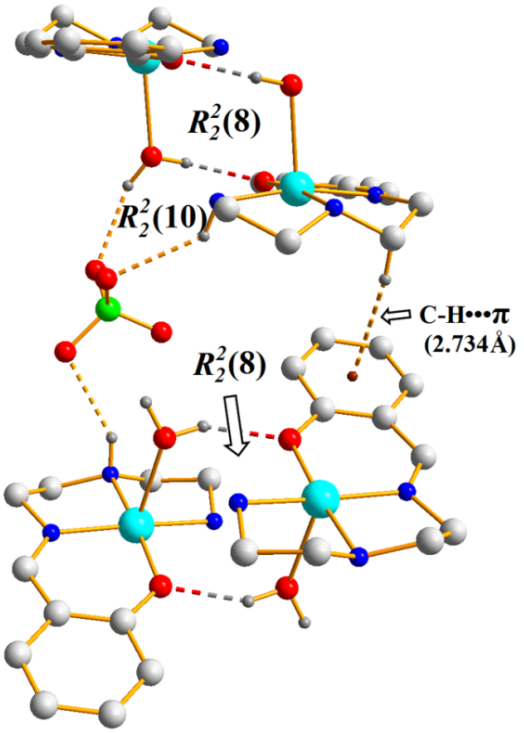

Fig. 3S. Supramolecular synthons of **1.**

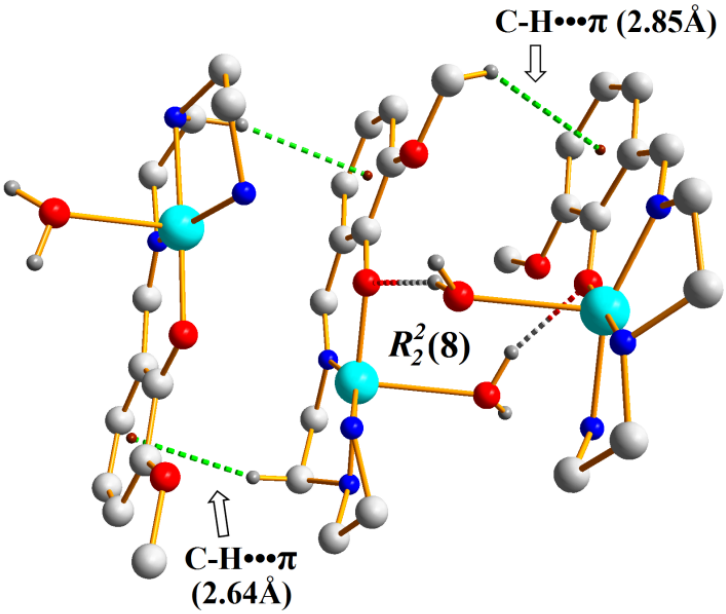

Fig. 4S. Supramolecular synthons of **2**.

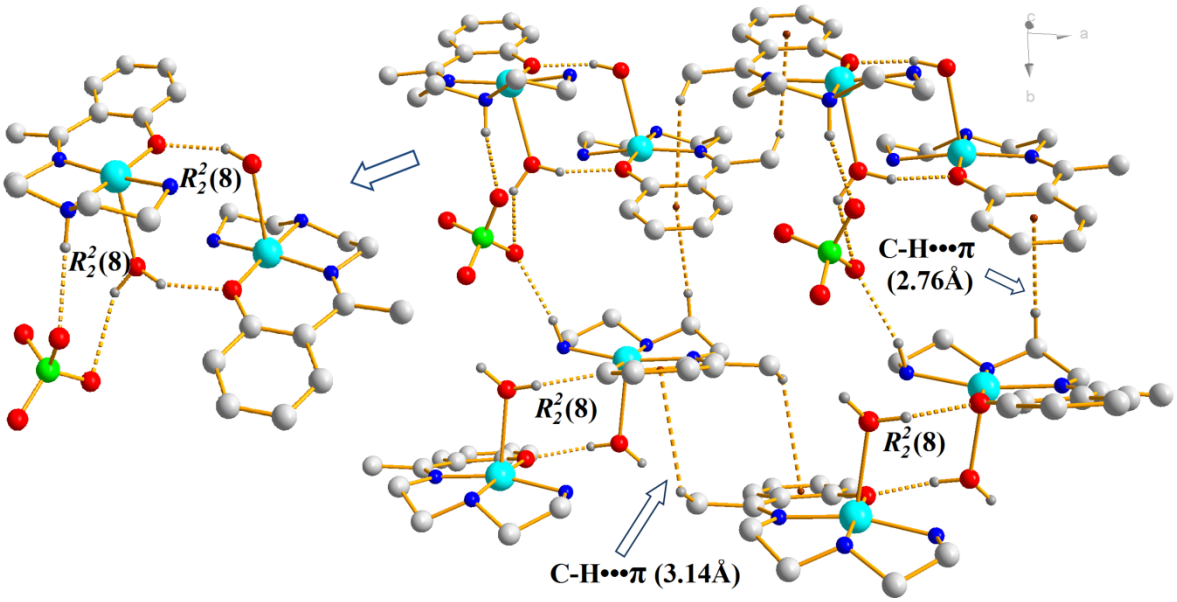

Fig. 5S. Supramolecular synthon of **3.**

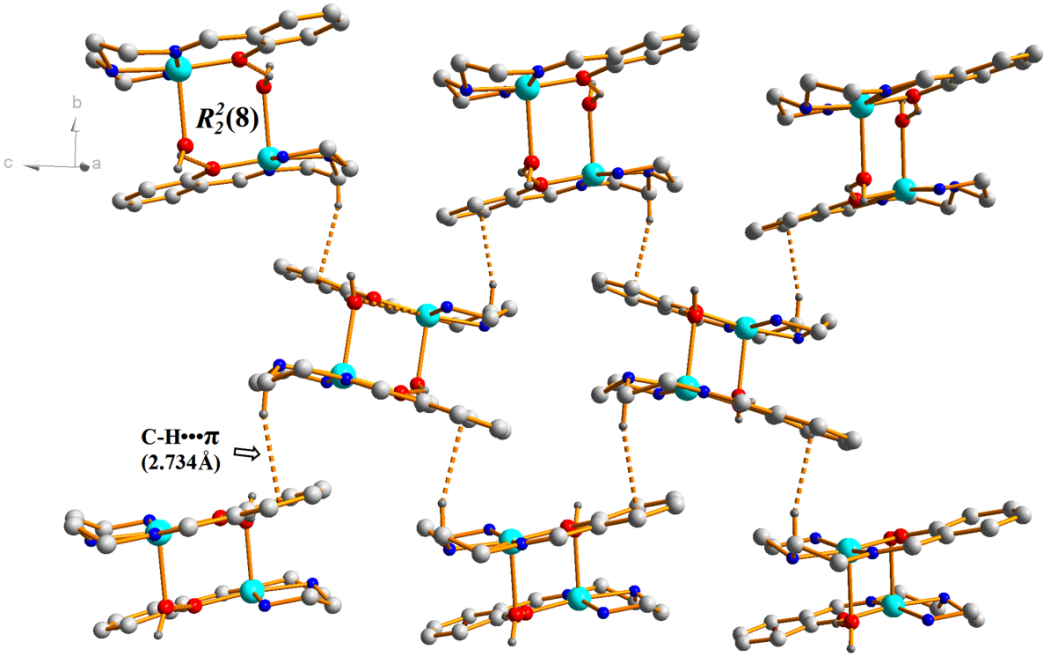

Fig. 6S. Supramolecular assembly of **1**.

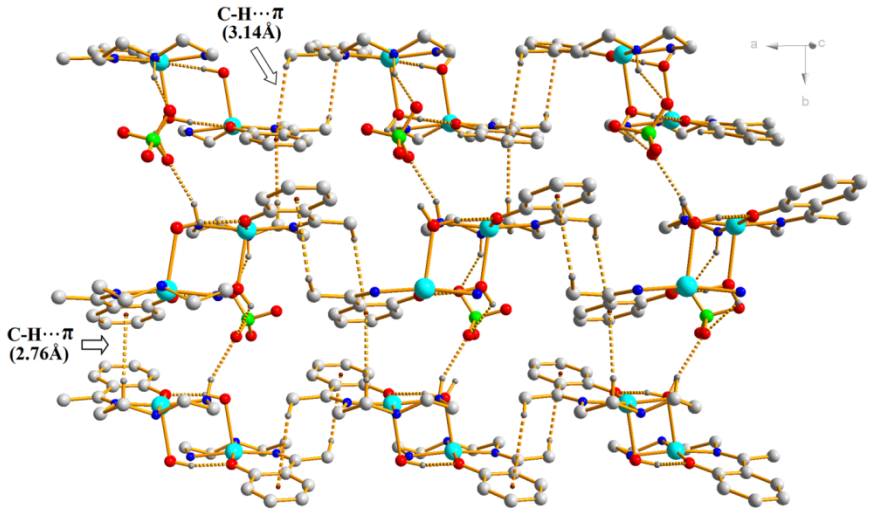

Fig.7S. The supramolecular assembly of **3**.

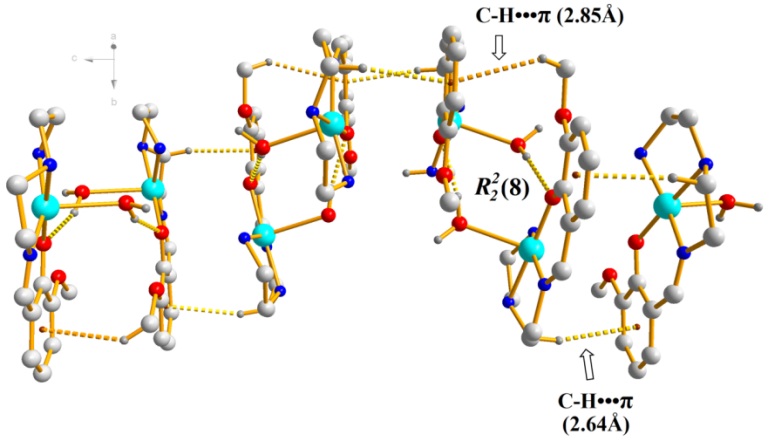

Fig. 8S. Supramolecular assembly of **2**.

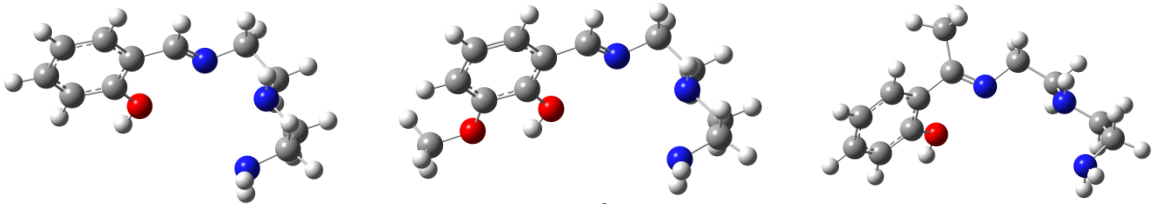

Fig. 9S. Optimized geometry of **HL**[1], **HL**[2]and **HL**[3] [B3LYP functional; basis set, 6-31G(d-p); using conductor-like polarizable continuum model (CPCM) in methanol].

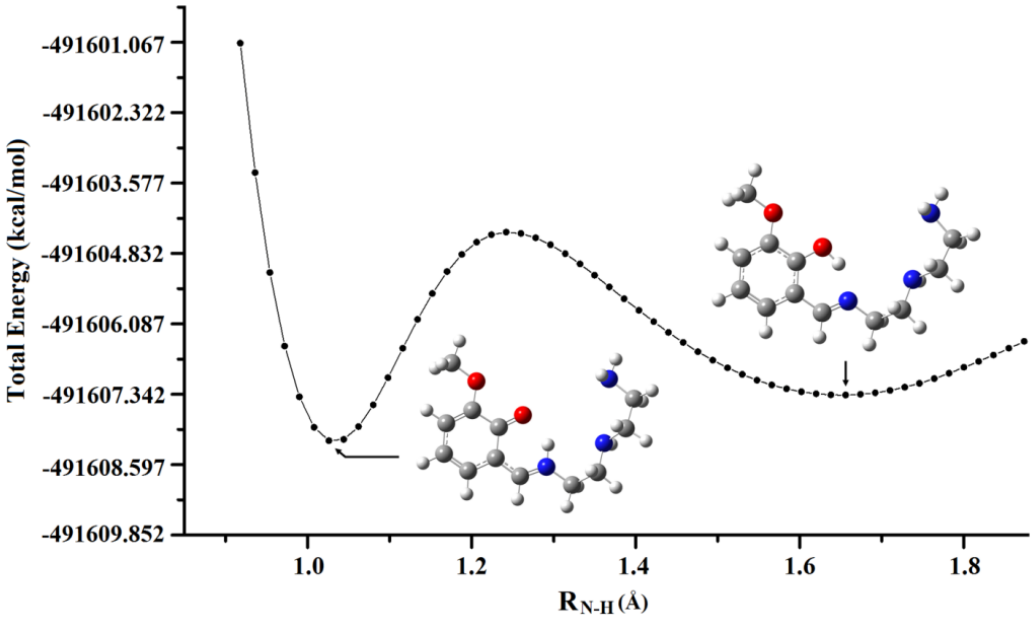

Fig. 10S. Potential energy curve at the ground S_0 state for **HL²** calculated at the DFT/B3LYP level.

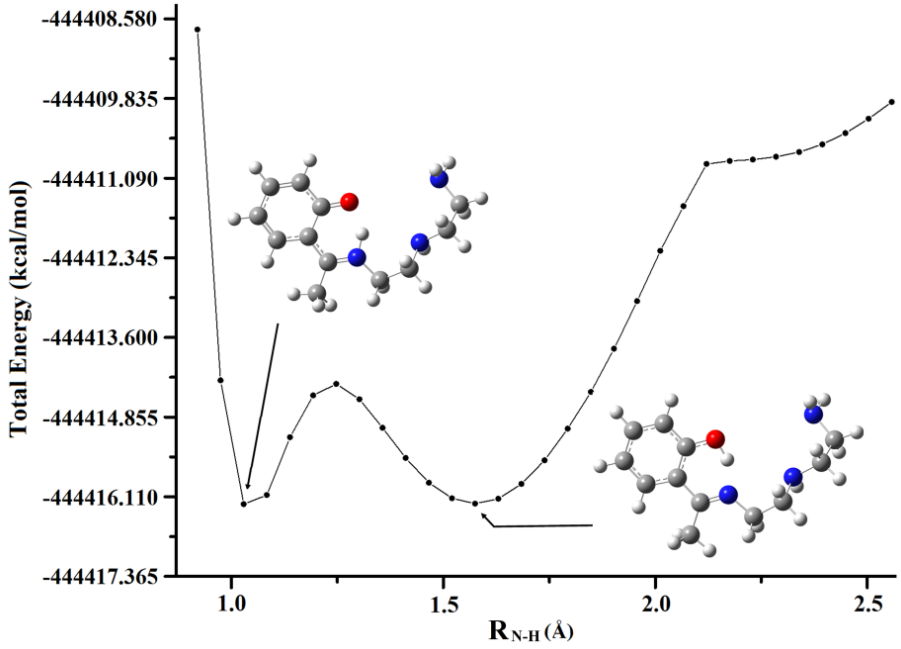

Fig. 11S. Potential energy curve at the ground S_0 state for **HL³** calculated at the DFT/B3LYP level.

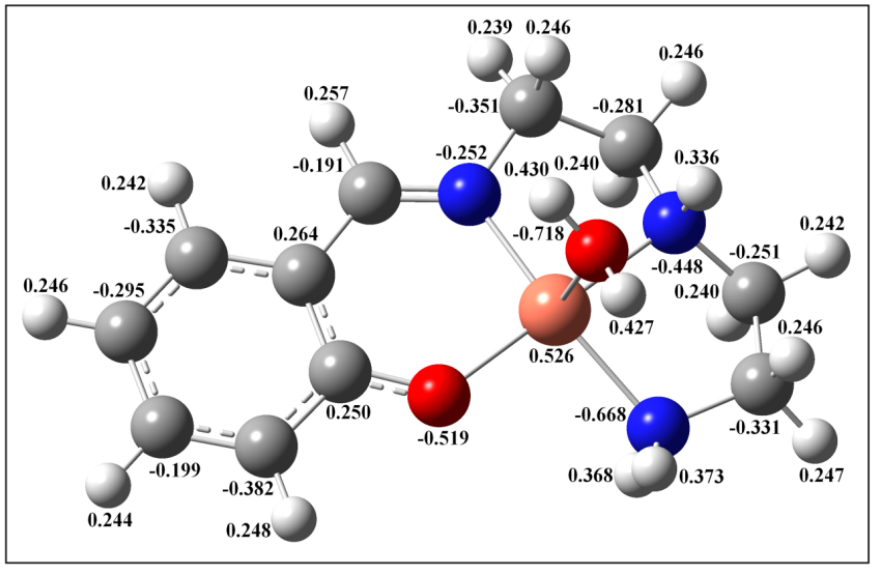

Fig. 12S. Optimized geometry of **1**with Mulliken charge distribution (B3LYP functional; in methanol; basis set LanL2DZ).

.

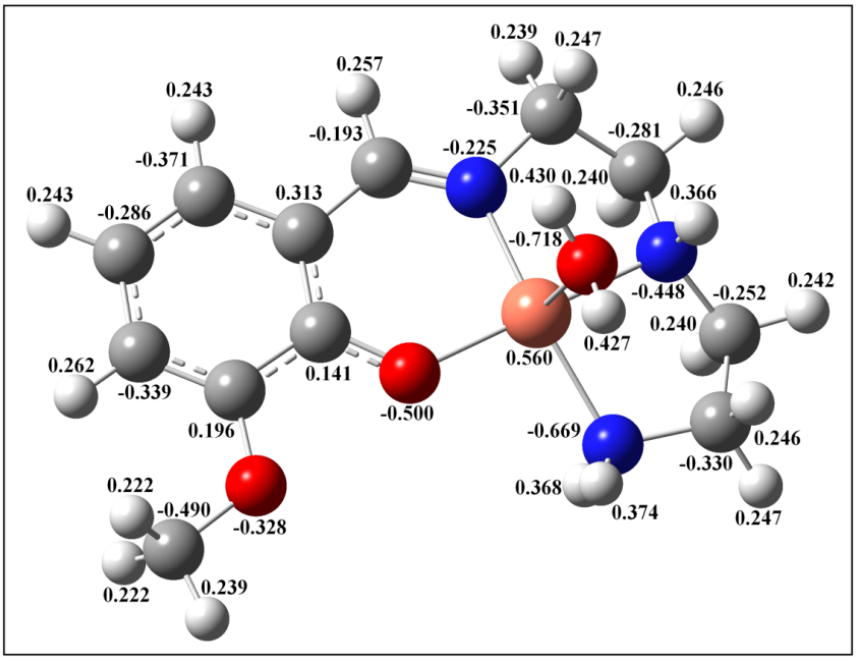

Fig. 13S. Optimized geometry of **2** with Mulliken charge distribution (B3LYP functional; in methanol; basis set LanL2DZ).

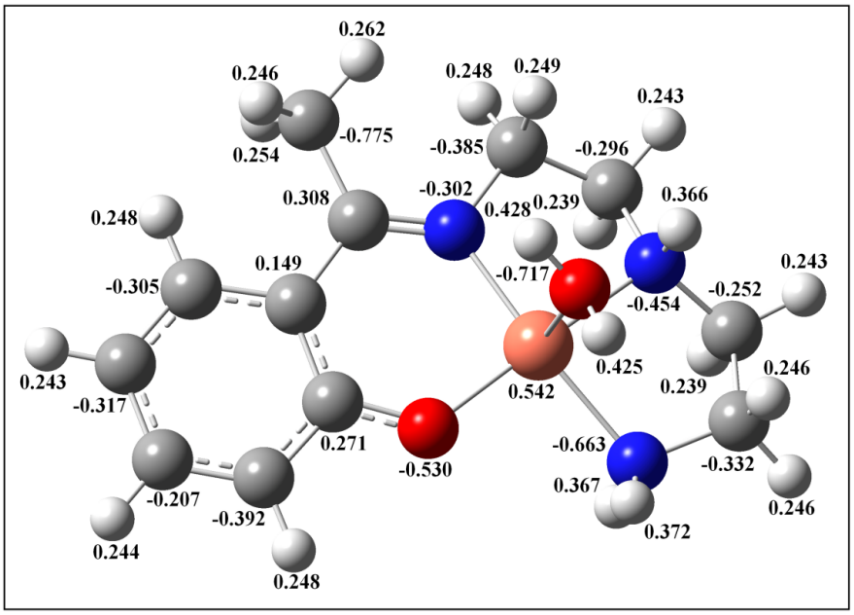

Fig. 14S. Optimized geometry of **3** with Mulliken charge distribution (B3LYP functional; in methanol; basis set LanL2DZ).

	MOs	B3LYPFunctional	B3PW91Functional	MPW1PW91Functional
Complex **1**	HOMO (α)	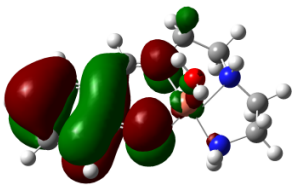 E = -5.97 eV, composition: L[1]97%,aqua0%,Cu 3%	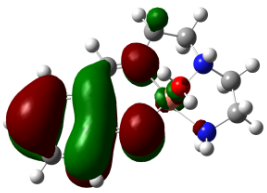 E = -6.06 eV, composition: L[1]97%,aqua0%,Cu 3%	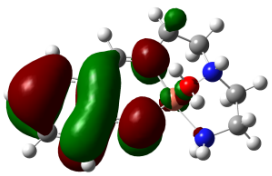 E = -6.24 eV, composition: L[1]97%,aqua0%,Cu 3%
	HOMO (β)	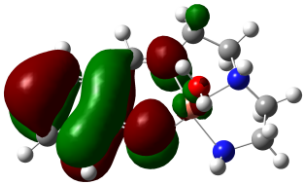 E = -5.92 eV,	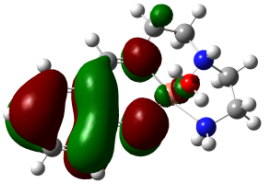 E = -6.01 eV,	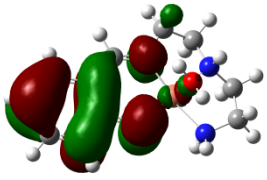 E = -6.18 eV,

		composition:	composition:	composition:
		$L^1$97%,aqua0%,Cu 3%	$L^1$97%,aqua0%,Cu 3%	$L^1$97%,aqua0%,Cu 3%
	LUMO (α)	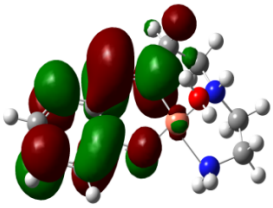	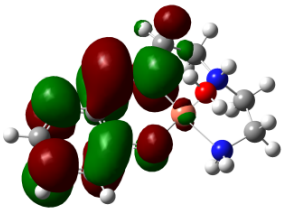	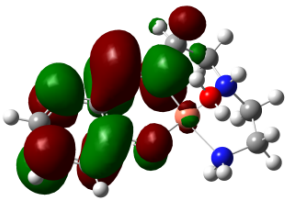
		E = -1.96eV,	E = -2.02 eV,	E = -1.81 eV,
		composition:	composition:	composition:
		$L^1$99%,aqua0%,Cu 1%	$L^1$99,aqua0%,Cu 1%	$L^1$97,aqua0%,Cu 3%
	LUMO (β)	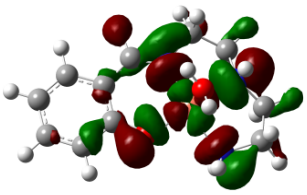	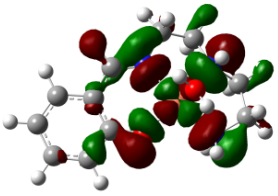	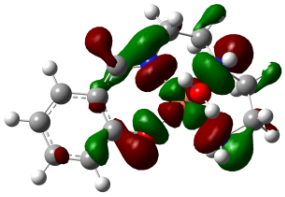
		E = -2.75 eV,	E = -2.80 eV,	E = -2.31 eV,
		composition:	composition:	composition:
		$L^1$40%,aqua0%,Cu 60%	$L^1$41,aqua0%,Cu 59%	$L^1$38,aqua0%,Cu 62%
Complex **2**	HOMO (α)	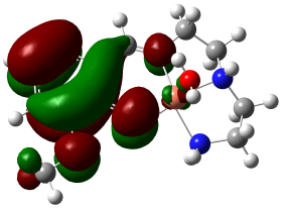	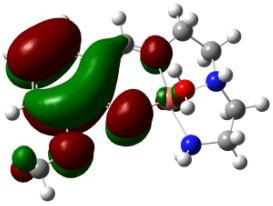	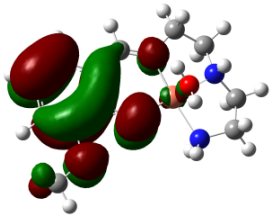
		E = -5.68 eV,	E = -5.75 eV,	E = -5.94 eV,
		composition:	composition:	composition:
		$L^2$98%,aqua0%,Cu 2%	$L^2$98%,aqua0%,Cu 2%	$L^2$98%,aqua0%,Cu 2%
	HOMO (β)	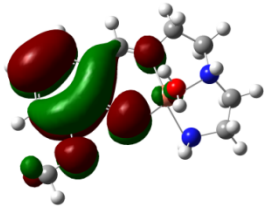	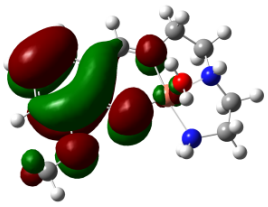	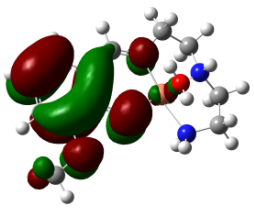

		E = -5.64eV, composition: $L^2$98%,aqua0%,Cu 2%	E = -5.71 eV, composition: $L^2$98%,aqua0%,Cu 2%	E = -5.90 eV, composition: $L^2$98%,aqua0%,Cu 2%
	LUMO (α)	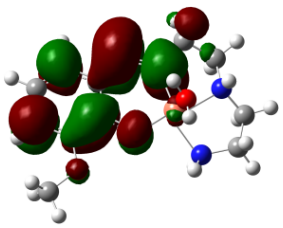	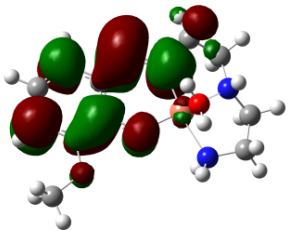	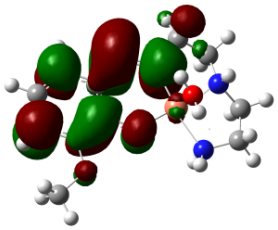
		E = -1.92 eV, composition: $L^2$99%,aqua0%,Cu 1%	E = -1.97 eV, composition: $L^2$99%,aqua0%,Cu 1%	E = -1.78 eV, composition: $L^2$99%,aqua0%,Cu 1%
	LUMO (β)	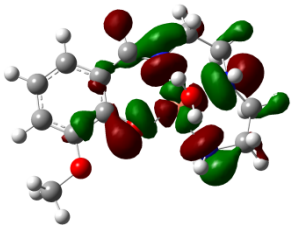	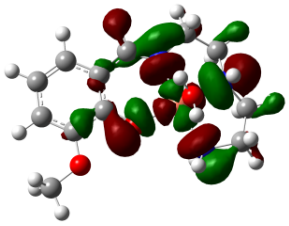	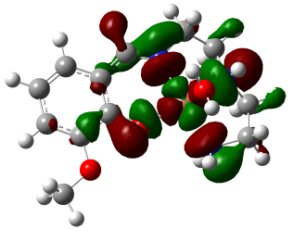
		E = -2.76 eV, composition: $L^2$40%,aqua0%,Cu 60%	E = -2.75 eV, composition: $L^2$41%,aqua0%,Cu 59%	E = -2.32 eV, composition: $L^2$38%,aqua0%,Cu 62%
Complex **3**	HOMO (α)	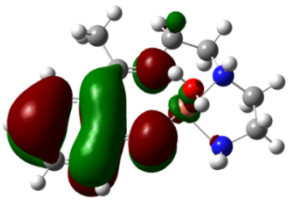	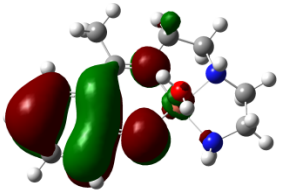	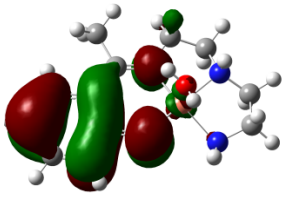
		E = -5.90 eV, composition: $L^3$97%,aqua0%,Cu 3%	E = -5.99 eV, composition: $L^3$97%,aqua0%,Cu 3%	E = -6.17 eV, composition: $L^3$97%,aqua0%,Cu 3%

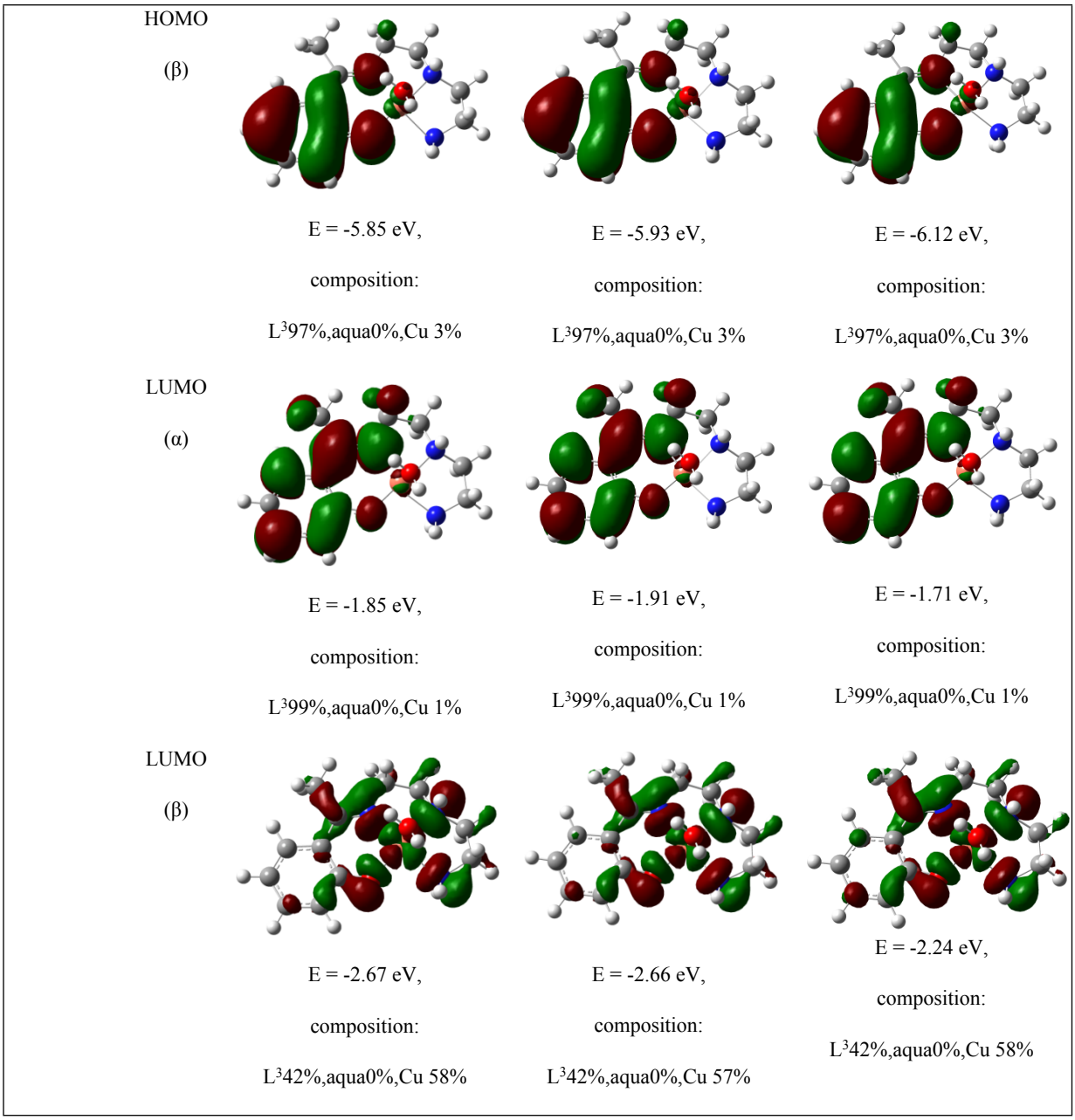

Fig.15S. Surface plot of frontier orbitals along with their energies and compositions of **1-3**,using B3LYP, B3PW91 and MPW1PW91 functionals.

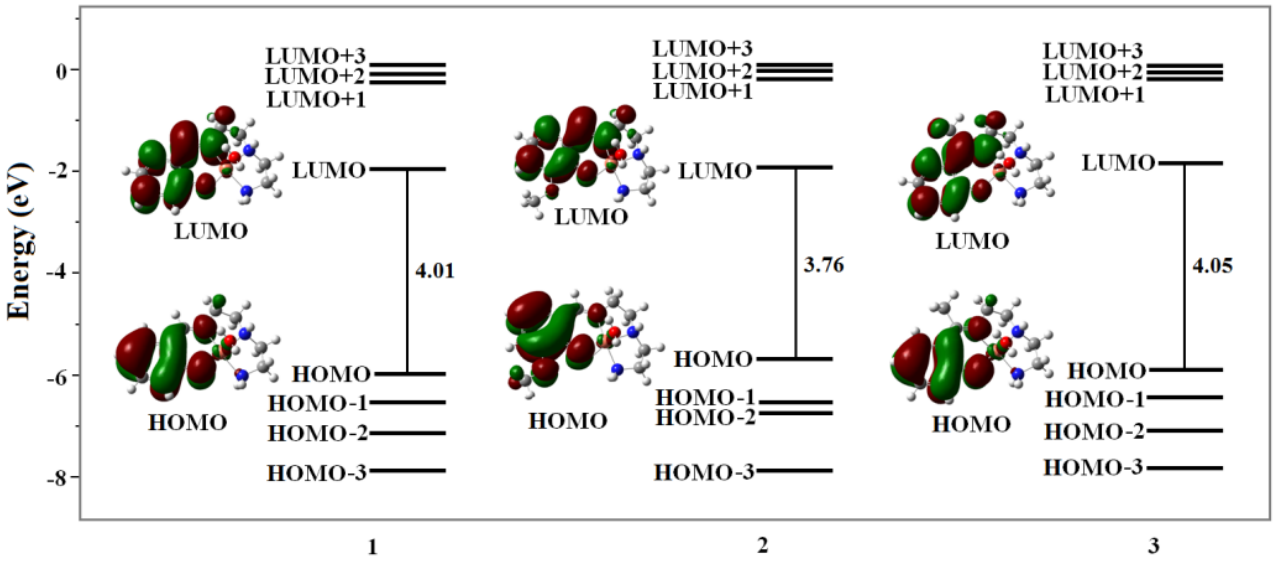

Fig. 16S. Calculated α molecular orbital energy level diagram of **1**, **2** and **3** [B3LYPfunctional; basis set LanL2DZ; using conductor-like polarizable continuum model (CPCM) in methanol].

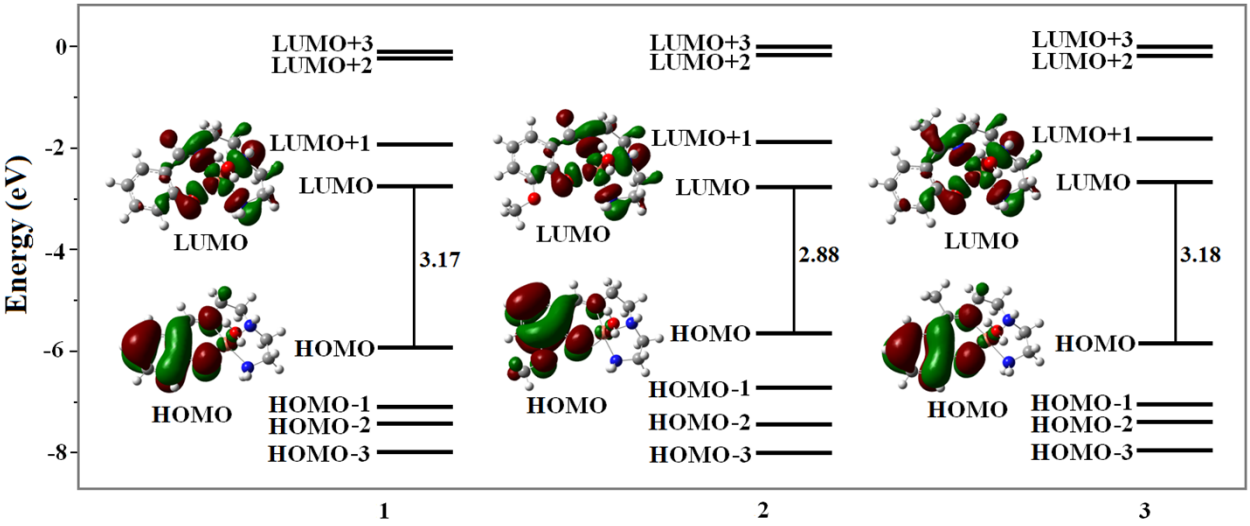

Fig. 17S. Calculated β molecular orbital energy level diagram of **1**, **2** and **3** [B3LYPfunctional; basis set LanL2DZ, using conductor-like polarizable continuum model (CPCM) in methanol].

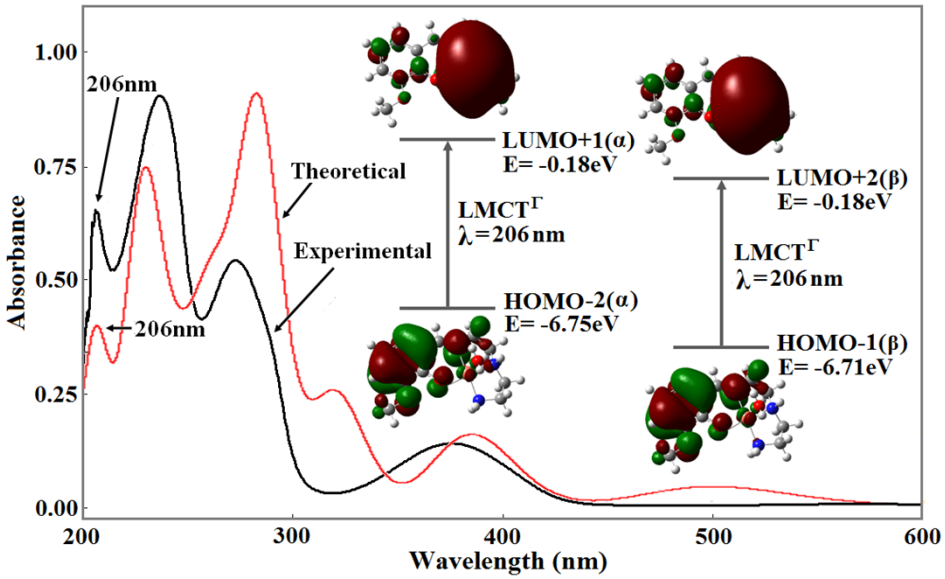

Fig. 18S. Theoretical (red line; B3LYP) and experimental (black line) electronic spectra (left) of **2**. The most prominent MOs involving transitions (right) and their diagrams.

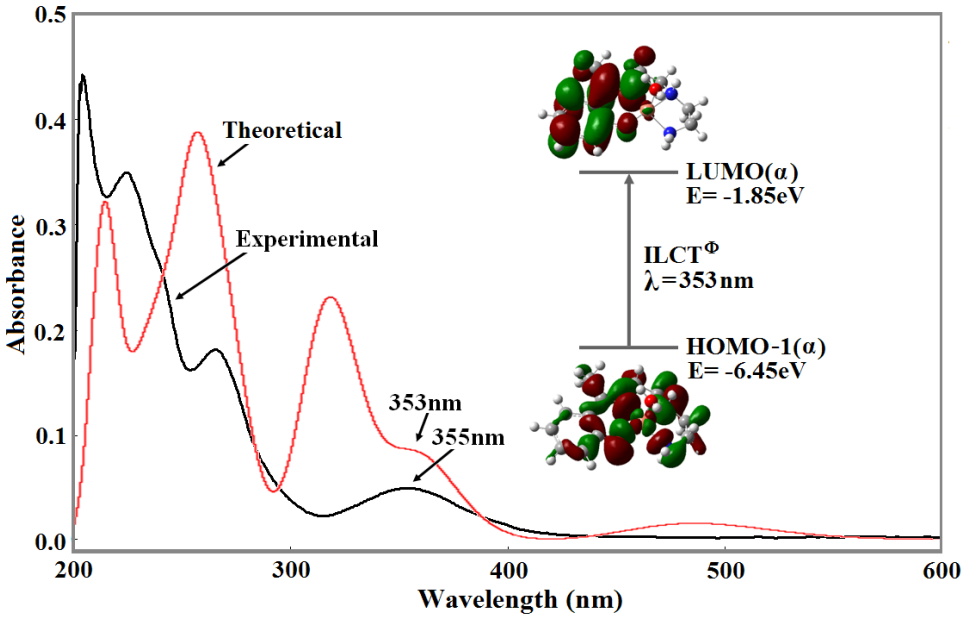

Fig. 19S. Theoretical (red line; B3LYP) and experimental (black line) electronic spectra (left) of **3**. The most prominent MOs involving transitions (right) and their diagrams.

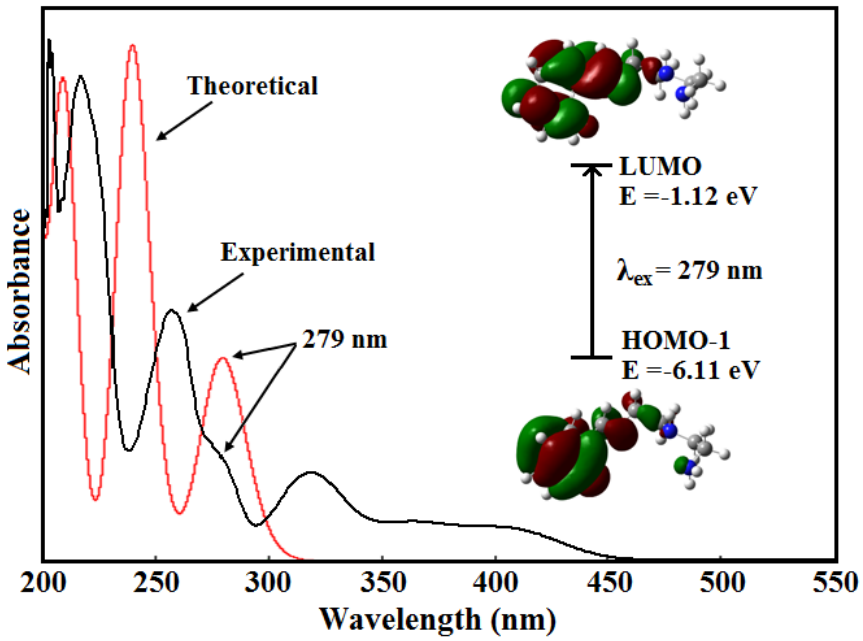

Fig. 20S. Theoretical (red line) and experimental (black line) electronic spectra (left) of HL^1. The most prominent MOs involving transitions (right) and their diagrams.

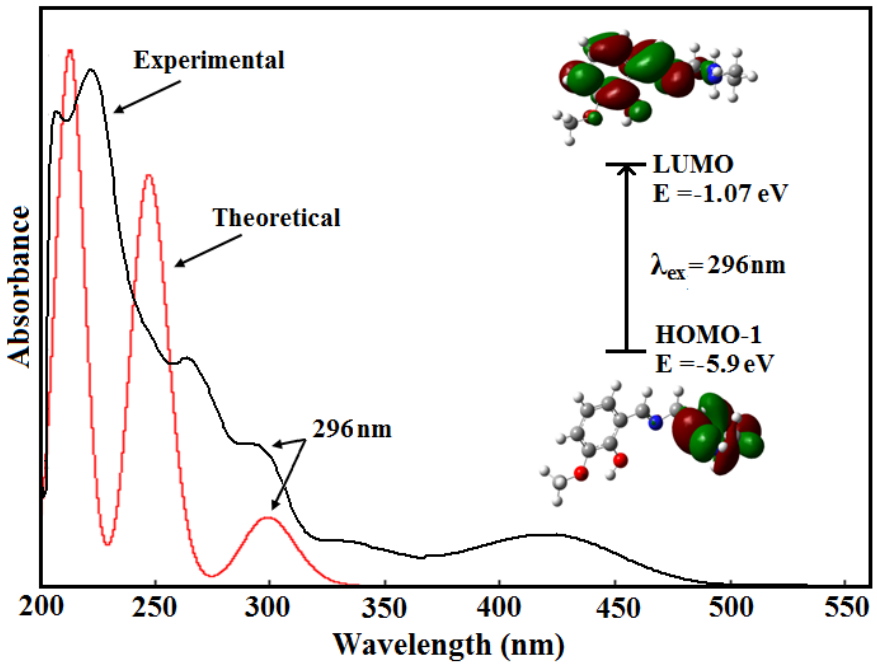

Fig. 21S. Theoretical (red line) and experimental (black line) electronic spectra (left) of HL^2. The most prominent MOs involving transitions (right) and their diagrams.

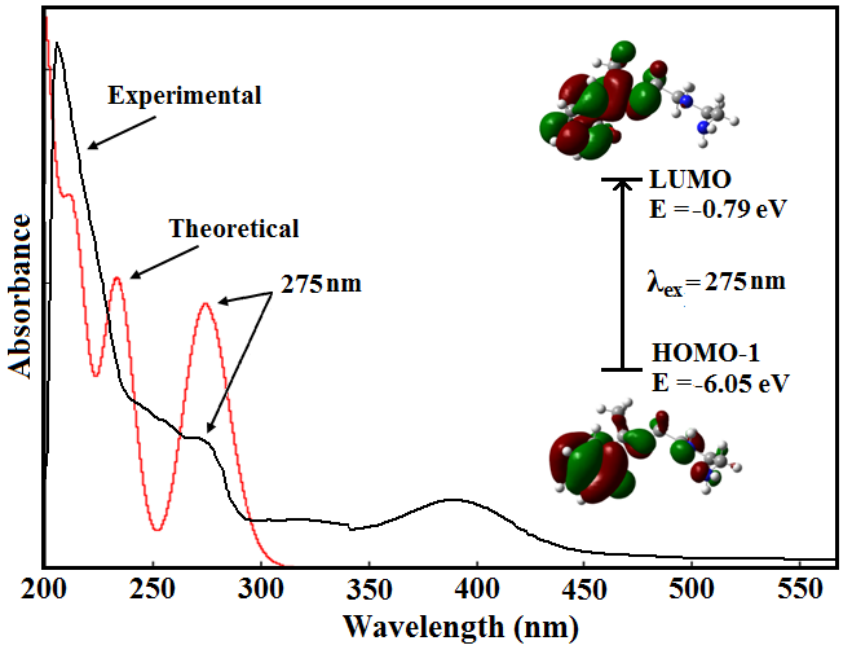

Fig. 22S. Theoretical (red line) and experimental (black line) electronic spectra (left) of HL^3. The most prominent MOs involving transitions (right) and their diagrams.

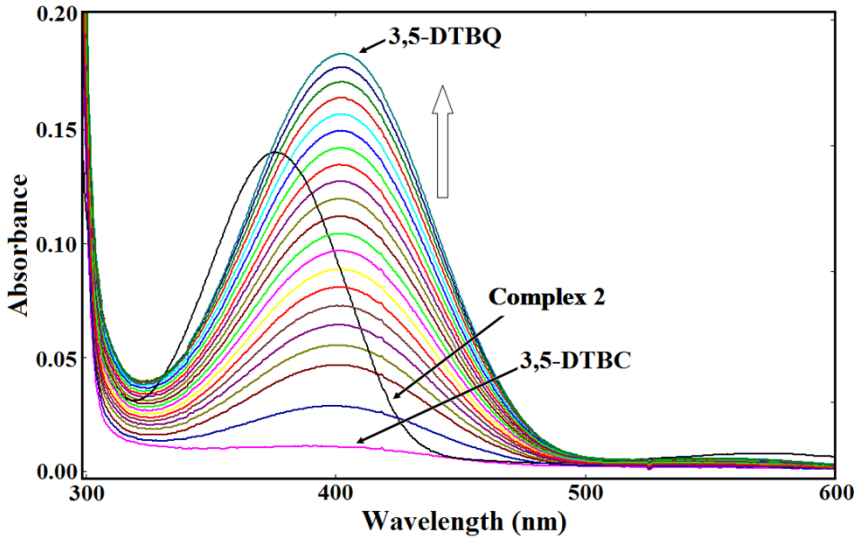

Fig. 23S. Increase in the 3,5-di-*tert*-butylquinone (3,5-DTBQ) band at 400 nm after addition of 10^{-4} M methanolic solution of complex **2** to 100 fold methanolic solution of 3,5-DTBC. The spectra were recorded at an interval of 5 min.

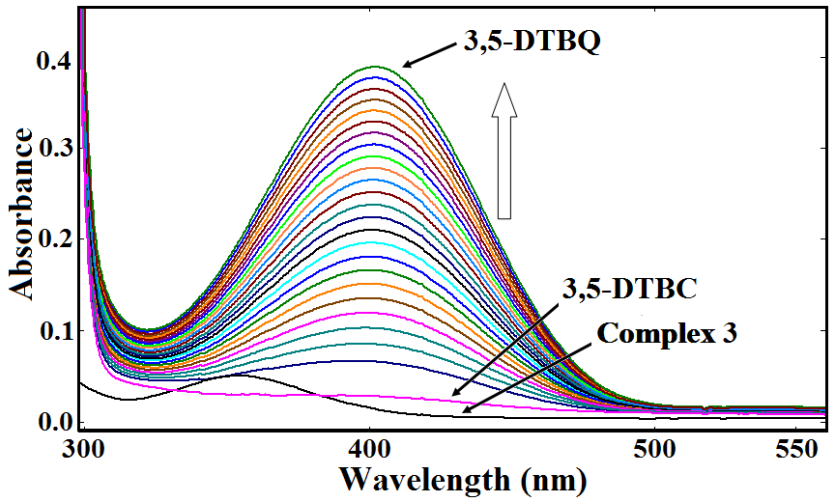

Fig. 24S. Increase in the 3,5-di-*tert*-butylquinone (3,5-DTBQ) band at 400 nm after addition of 10^{-4} M methanolic solution of complex **3** to 100 fold methanolic solution of 3,5-DTBC. The spectra were recorded at an interval of 5 min.

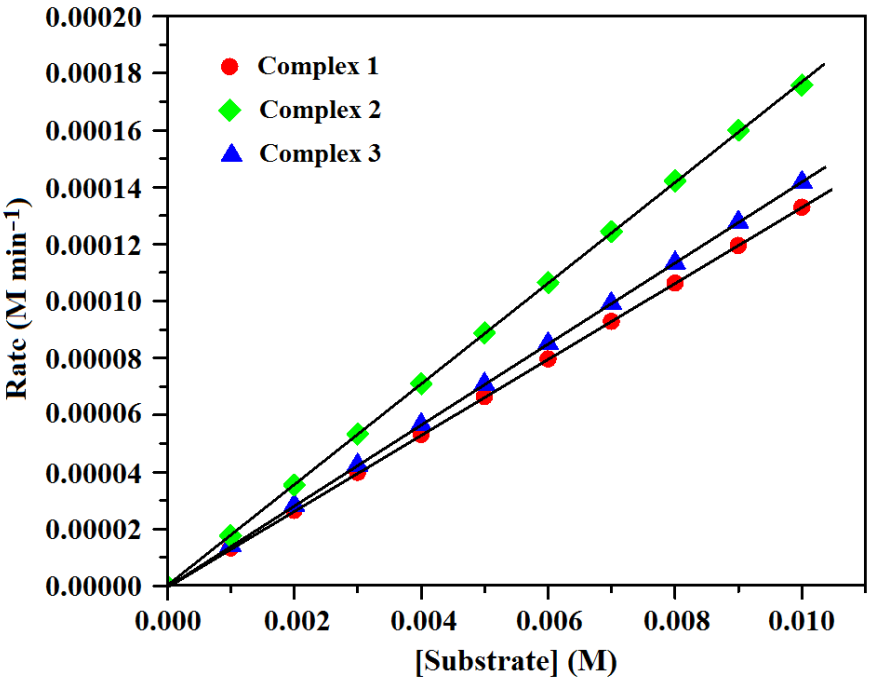

Fig. 25S. Plot of rate *vs* substrate concentration for complexes **1**, **2** and **3**.

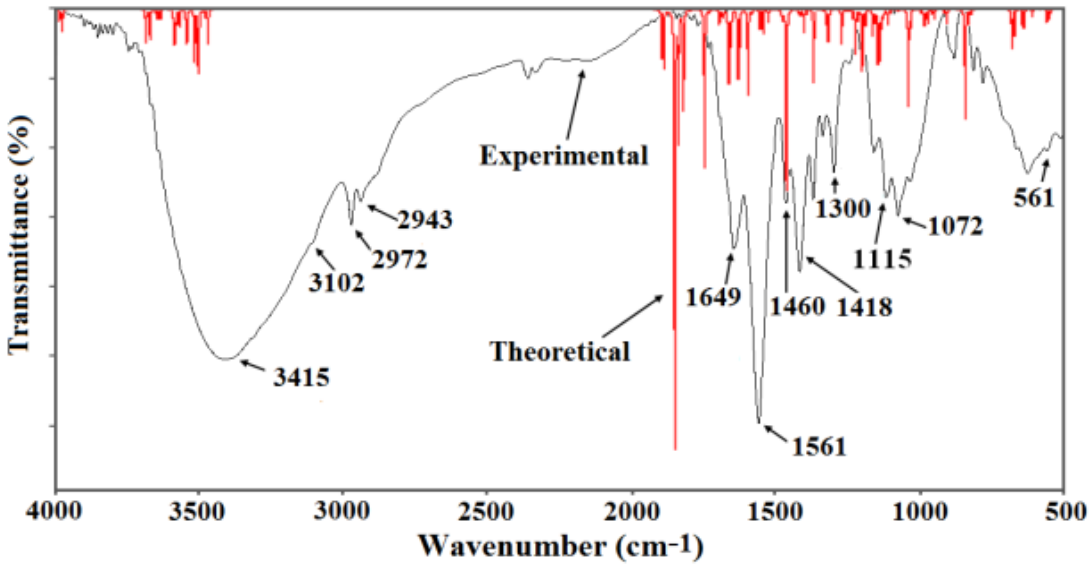

Fig.26S. Theoretical [red line, using basis set LanL2DZ, in methanol] and experimental [black line, as KBr pellet] IR spectra of complex **1**.

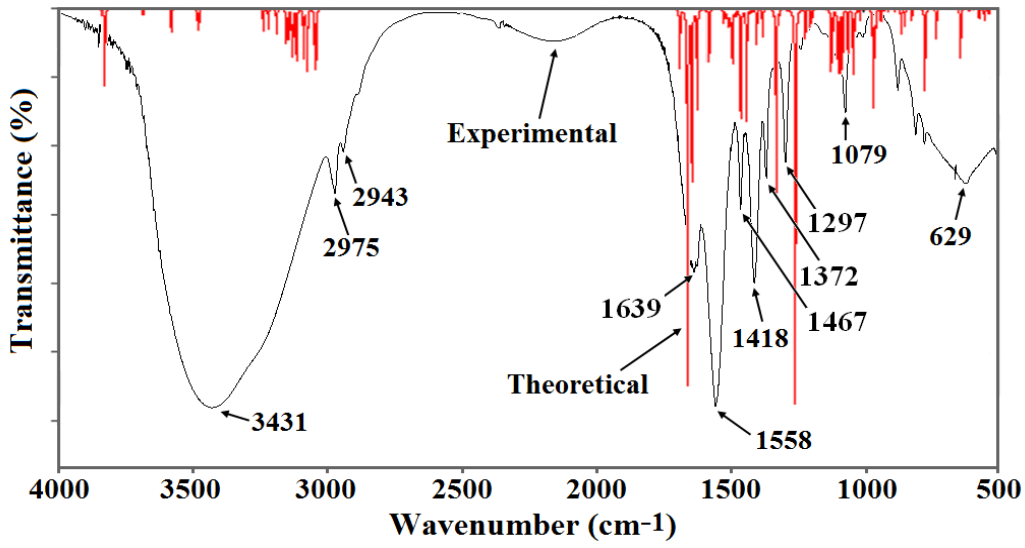

Fig.27S. Theoretical [red line, using basis set LanL2DZ, in methanol] and experimental [black line, as KBr pellet] IR spectra of complex **2**.

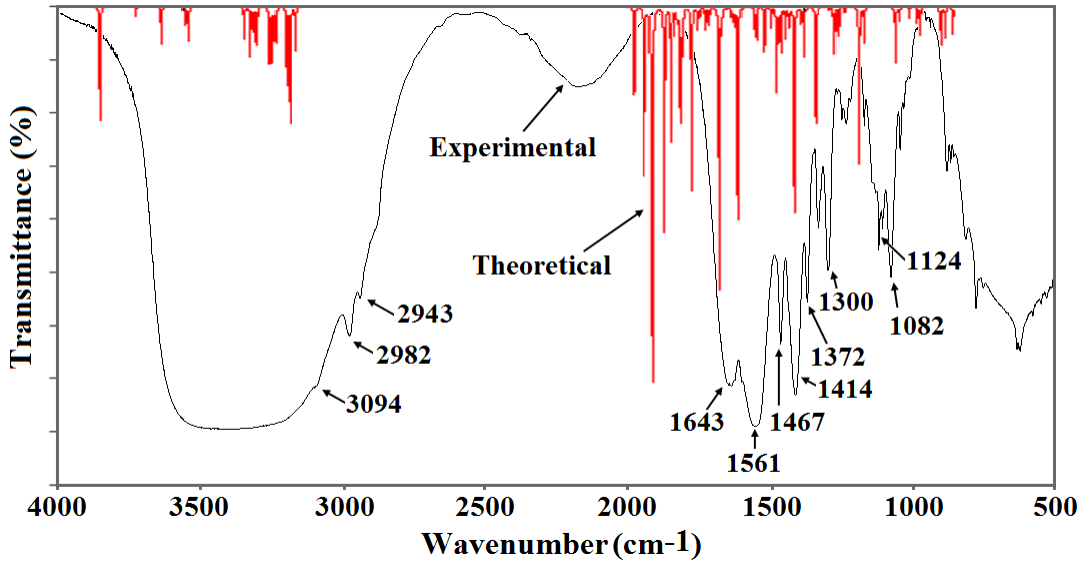

Fig.28S. Theoretical [red line, using basis set LanL2DZ, in methanol] and experimental [black line, as KBr pellet] IR spectra of complex **3**.

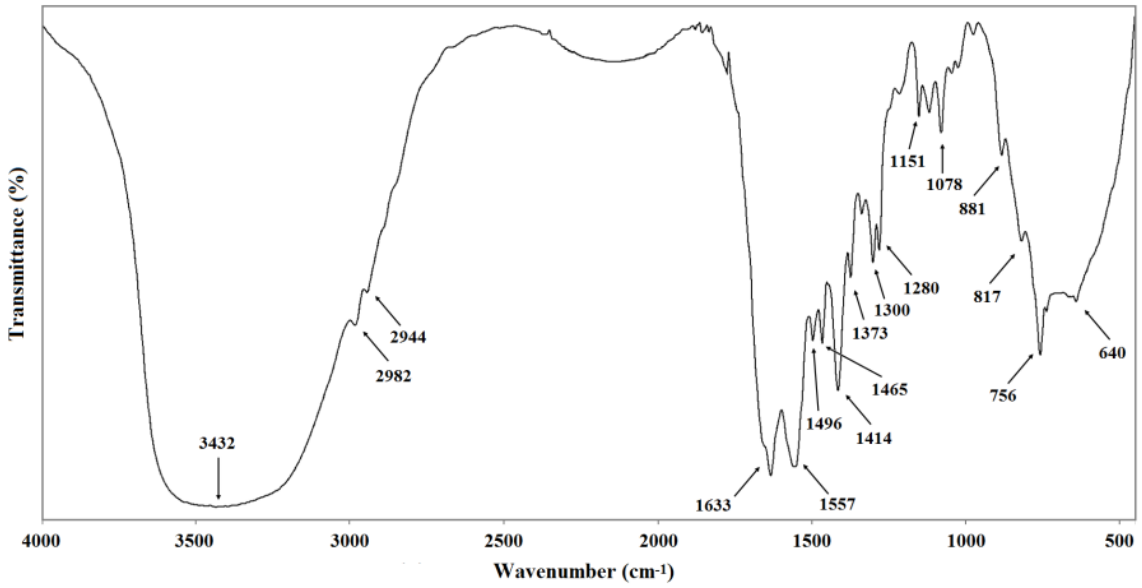

Fig.29S. IR spectra of **HL**[1].

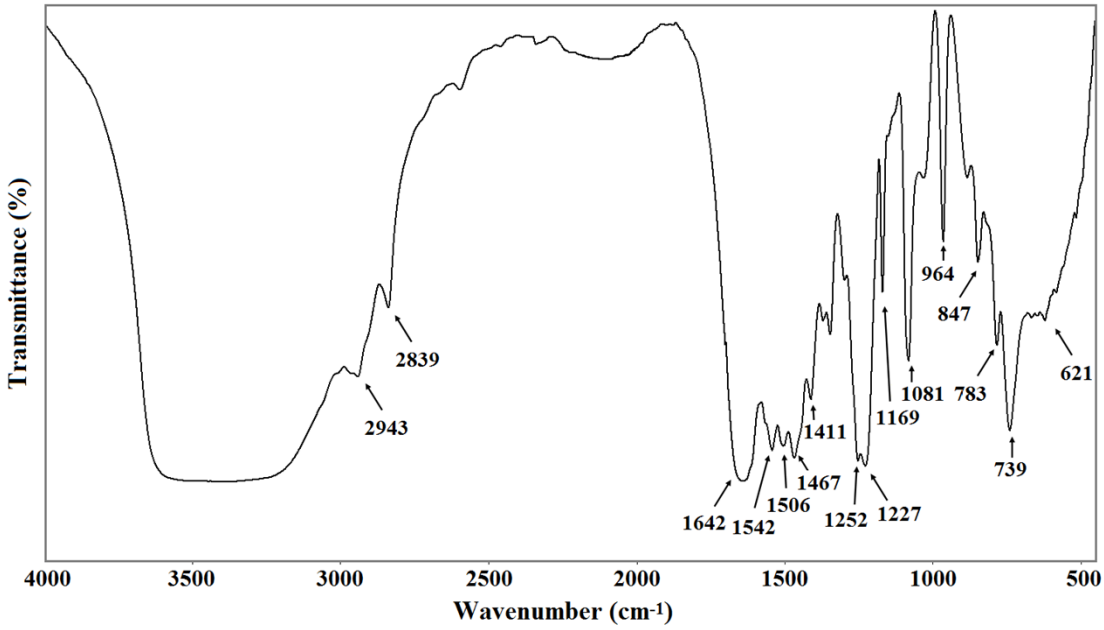

Fig.30S. IR spectra of **HL²**.

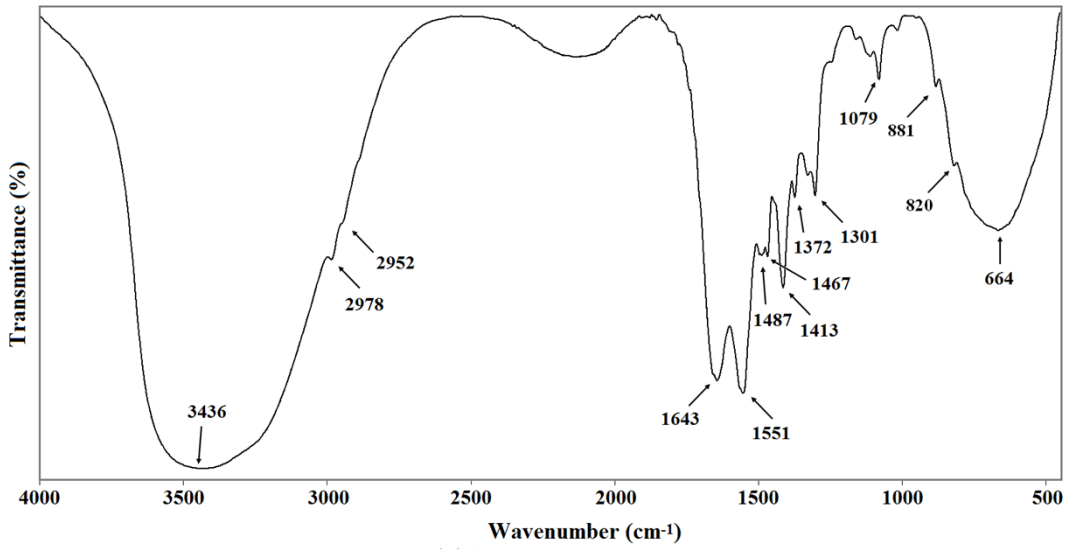

Fig.31S. IR spectra of **HL³**.

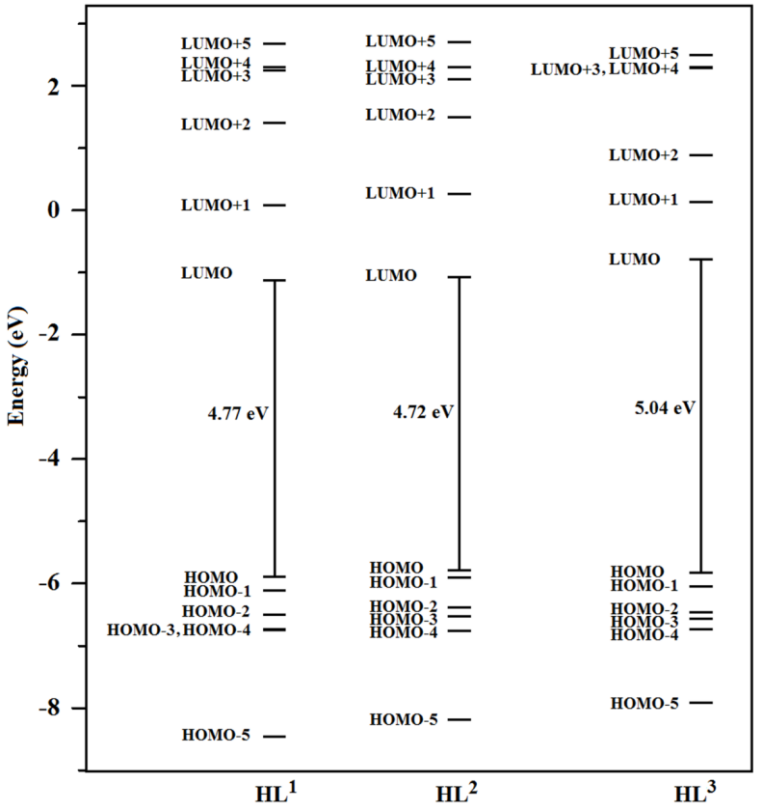

Fig. 32S. Calculated molecular orbital energy level diagram of HL^1, HL^2 and HL^3 [B3LYP functional; basis set, 6-31G(d-p); using conductor-like polarizable continuum model (CPCM) in methanol].

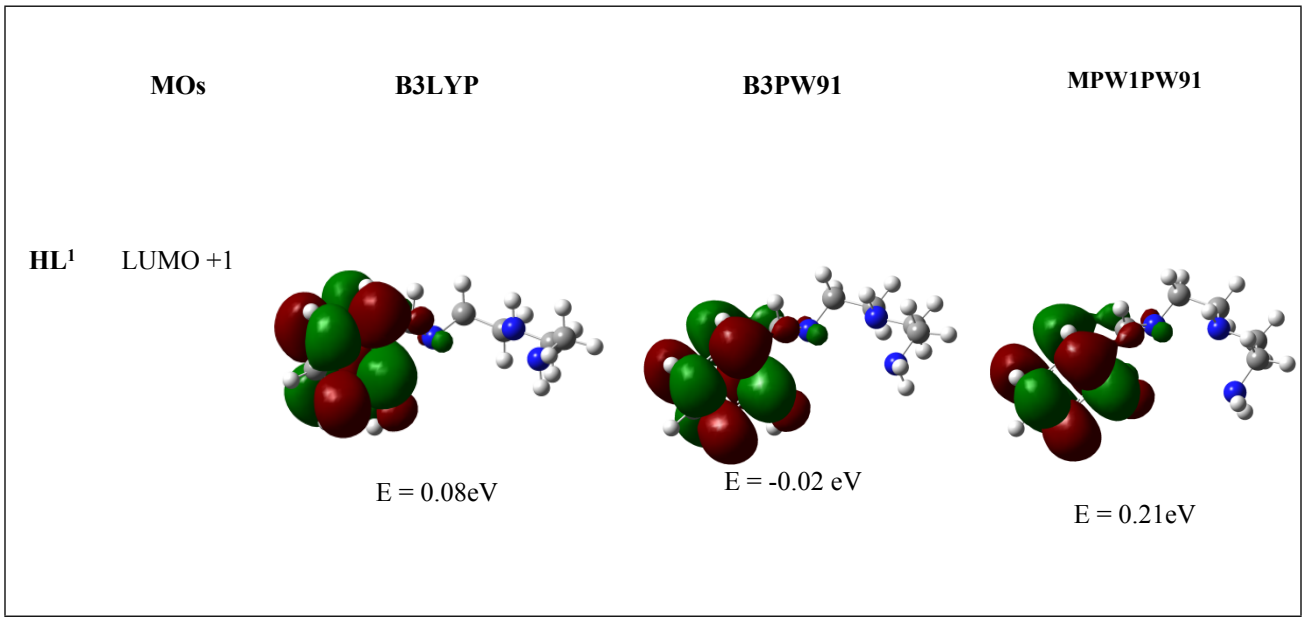

	LUMO	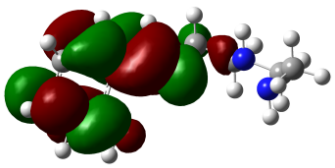	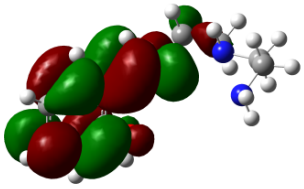	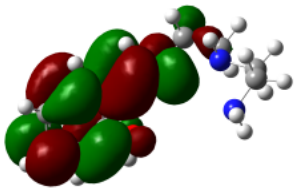
		E= -1.12	E = -1.22 eV	E = -1.01eV
	HOMO	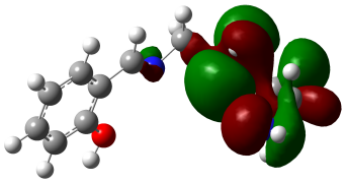	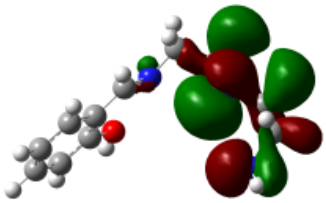	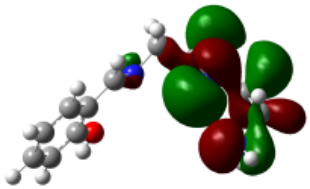
		E =-5.89 eV	E = -5.93eV	E = -6.20eV
	HOMO -1	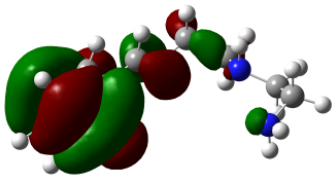		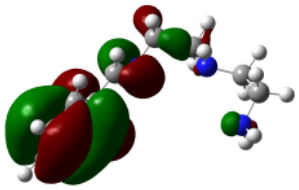
		E = -6.11 eV	E = -6.22 eV	E = -6.41 eV
HL²	LUMO +1	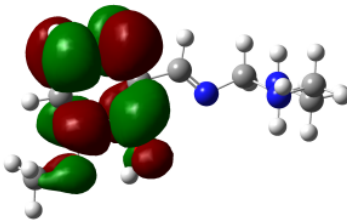	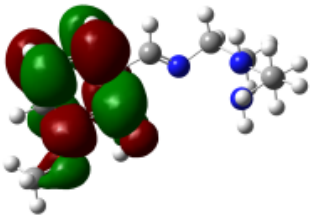	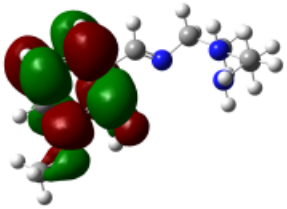
		E= 0.26	E= 0.18	E=0.40

	LUMO	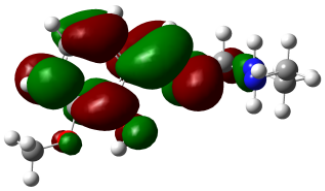 E= -1.07	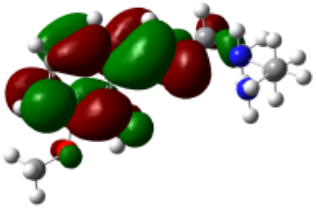 E= -1.17	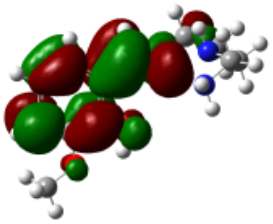 E= -0.96
	HOMO	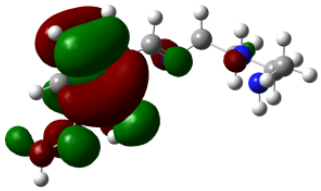 E= -5.79	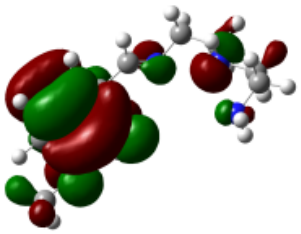 E= -5.9	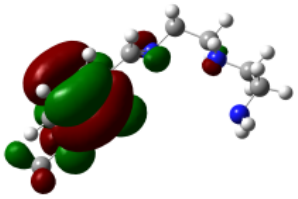 E= -6.09
	HOMO -1	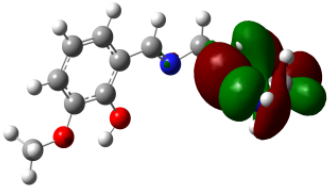 E= -5.90	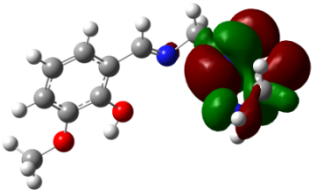 E= -5.94	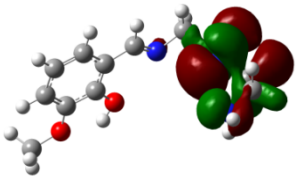 E= -6.21
HL³	LUMO + 1	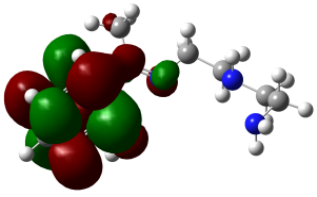 E = 0.14 eV	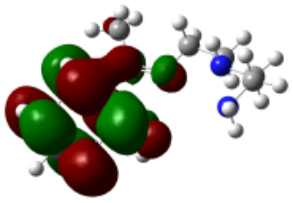 E = 0.06eV	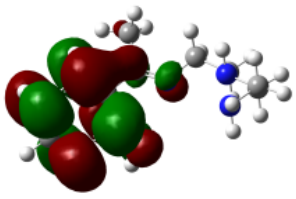 E = 0.28 eV

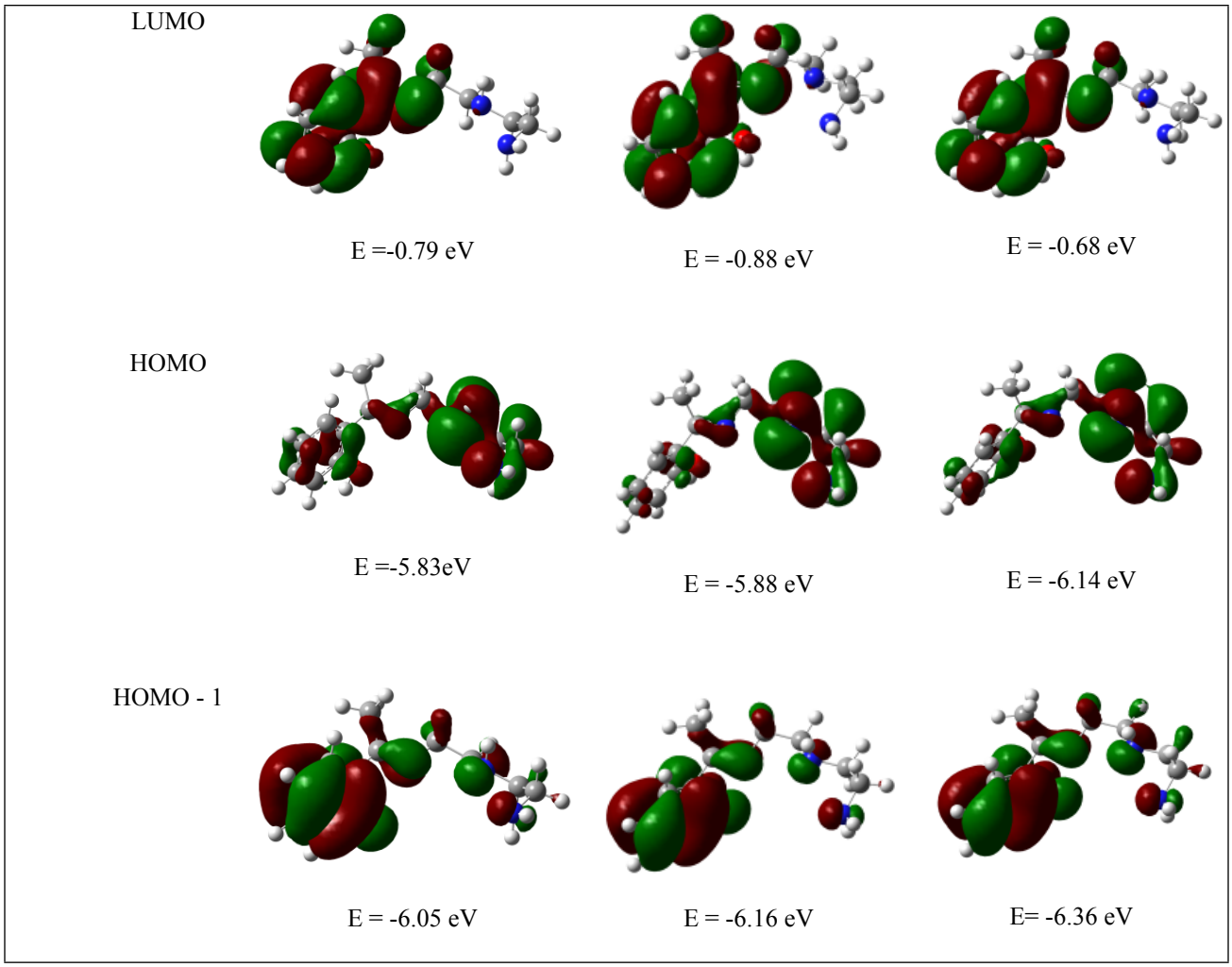

Fig.33S. Surface plot of frontier orbitals along with their energies and compositions of HL^1, HL^2 and HL^3, using B3LYP, B3PW91 and MPW1PW91 functionals.

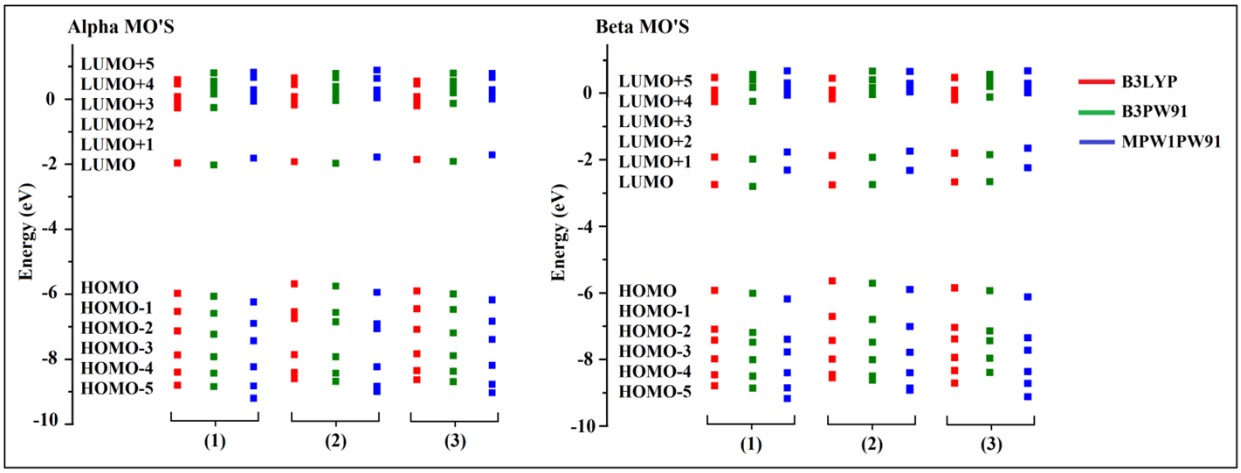

Fig. 34S. Calculated molecular orbital energy level diagram of **1-3**, using B3LYP, B3PW91 and MPW1PW91 functionals. [red, B3LYP; green B3PW91; blue, MPW1PW91].

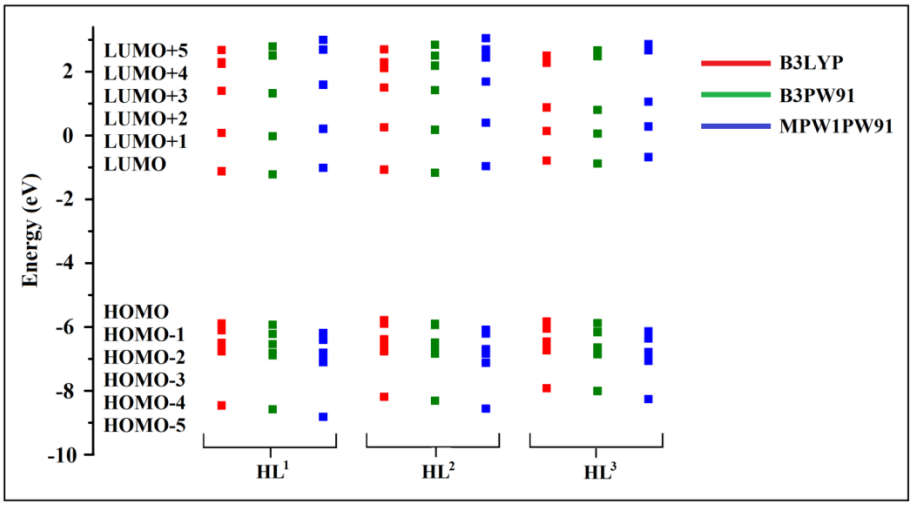

Fig. 35S. Calculated molecular orbital energy level diagram of HL^1, HL^2 and HL^3, using B3LYP, B3PW91 and MPW1PW91 functionals. [Basis set, 6-31 G (d-p); using conductor-like polarizable continuum model (CPCM) in methanol]. [red, B3LYP; green B3PW91; blue, MPW1PW91].

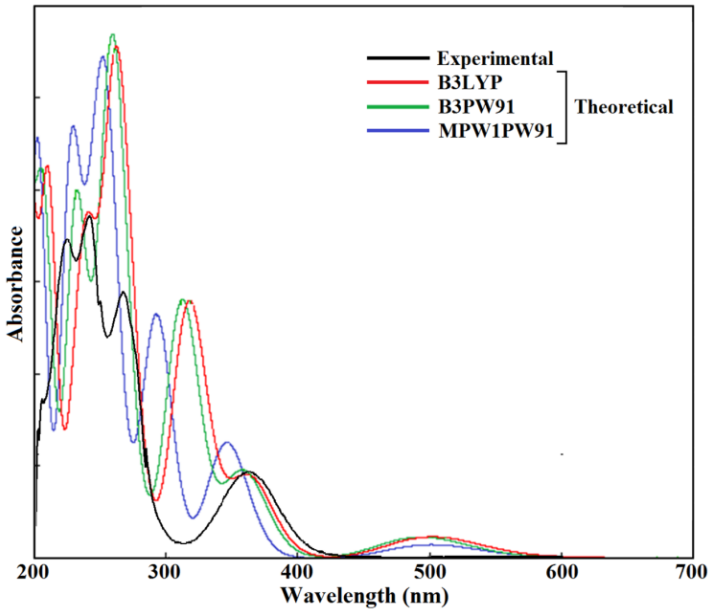

Fig. 36S. Experimental (black line) and theoretical (red, green and blue line, using B3LYP, B3PW91, MPW1PW91 functionals, respectively) electronic spectra of complex **1**.

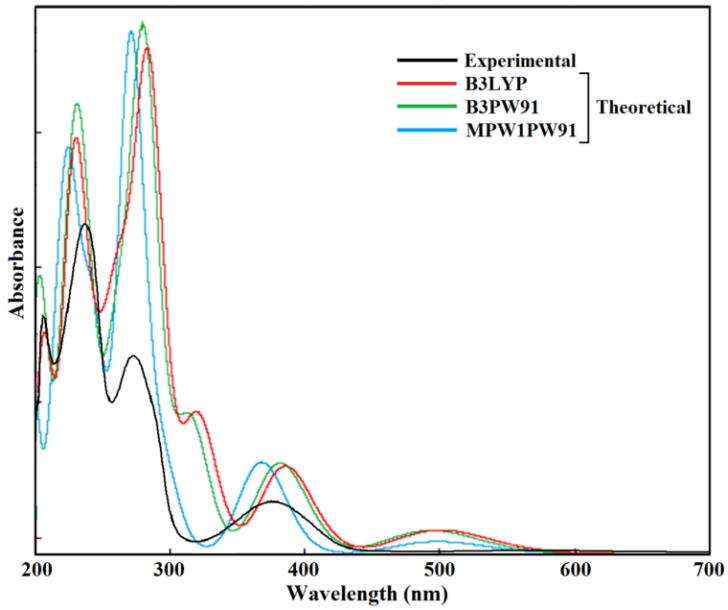

Fig.37S. Experimental (black line) and theoretical (red, green and blue line, using B3LYP, B3PW91, MPW1PW91 functionals, respectively) electronic spectra of complex **2**.

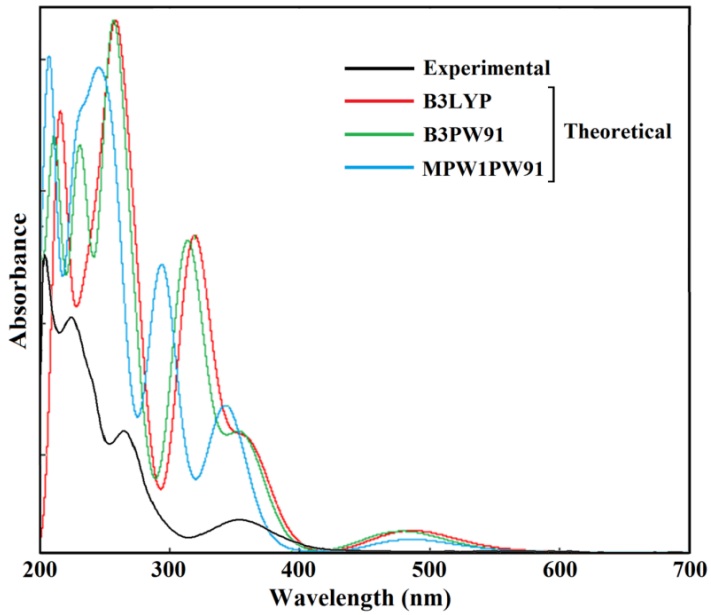

Fig. 38S. Experimental (black line) andtheoretical (red, green and blue line, using B3LYP, B3PW91, MPW1PW91 functionals, respectively) electronic spectra of complex **3**.

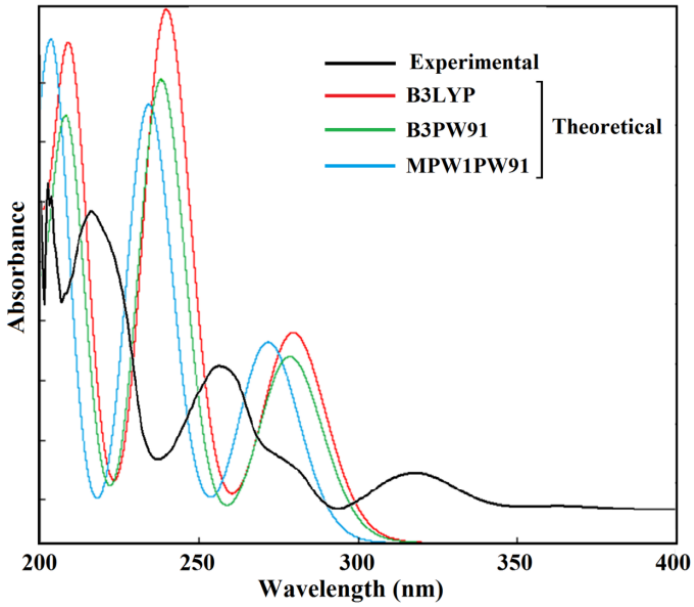

Fig. 39S. Experimental (black line) and theoretical (red, green and blue line, using B3LYP, B3PW91, MPW1PW91 functionals, respectively) electronic spectra of complex HL^1.

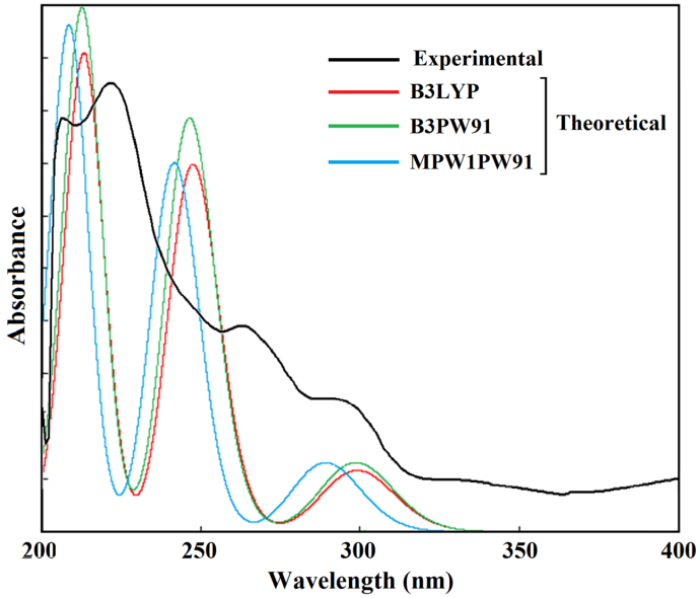

Fig.40S. Experimental (black line) and theoretical (red, green and blue line, using B3LYP, B3PW91, MPW1PW91 functionals, respectively) electronic spectra of complex HL^2.

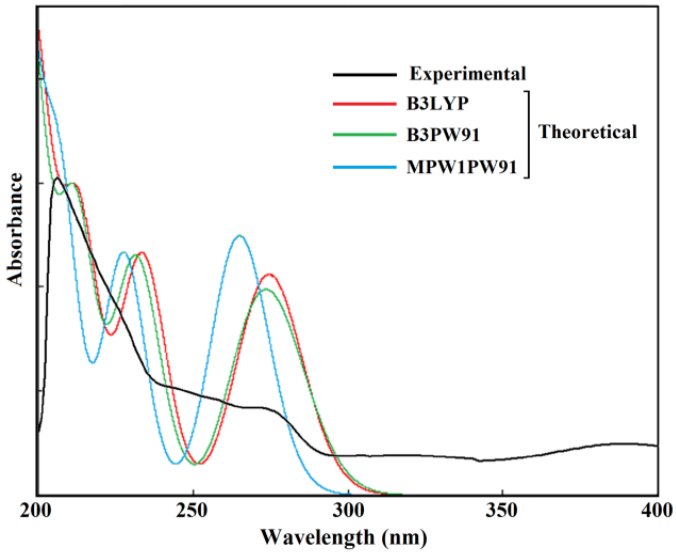

Fig. 41S. Experimental (black line) and theoretical (red, green and blue line, using B3LYP, B3PW91, MPW1PW91 functionals, respectively) electronic spectra of complex HL^3.

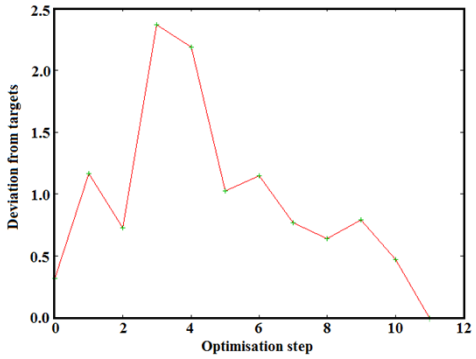

Fig.42S. Deviation from target vs. optimization step of **1 [**using conductor-like polarizable continuum model (CPCM) in methanol; basis set, LanL2DZ].

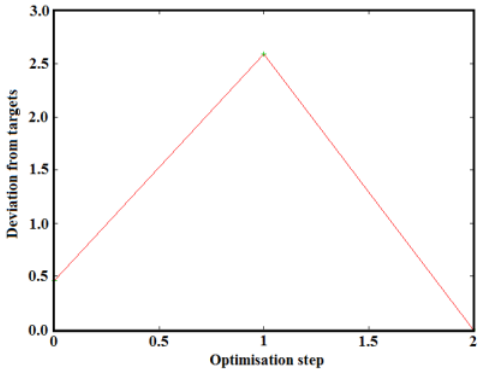

Fig.43S. Deviation from target vs. optimization step of **2[**using conductor-like polarizable continuum model (CPCM) in methanol; basis set, LanL2DZ].

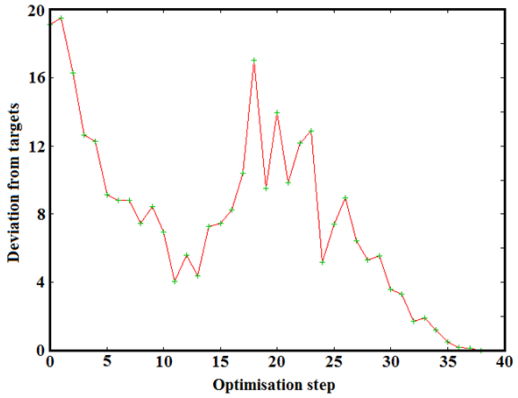

Fig.44S. Deviation from target vs. optimization step of **3 [**using conductor-like polarizable continuum model (CPCM) in methanol; basis set, LanL2DZ].

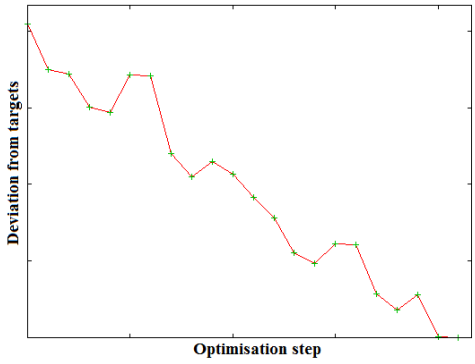

Fig.45S. Deviation from target vs. optimization step of HL[1] [using conductor-like polarizable continuum model (CPCM) in methanol; basis set, 6-31G (d-p)].

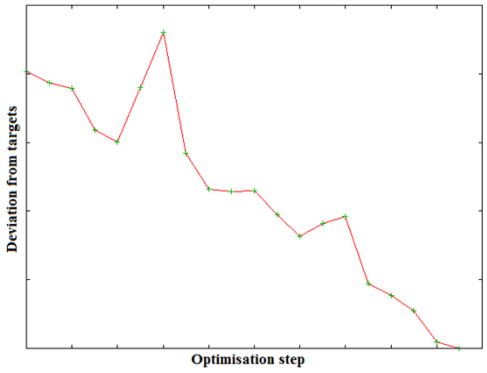

Fig. 46S. Deviation from target vs. optimization step of HL^2 [using conductor-like polarizable continuum model (CPCM) in methanol; basis set, 6-31G(d-p)].

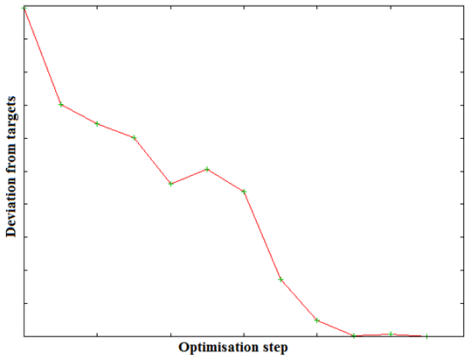

Fig.47S. Deviation from target vs. optimization step of HL^3[using conductor-like polarizable continuum model (CPCM) in methanol; basis set, 6-31G (d-p)].

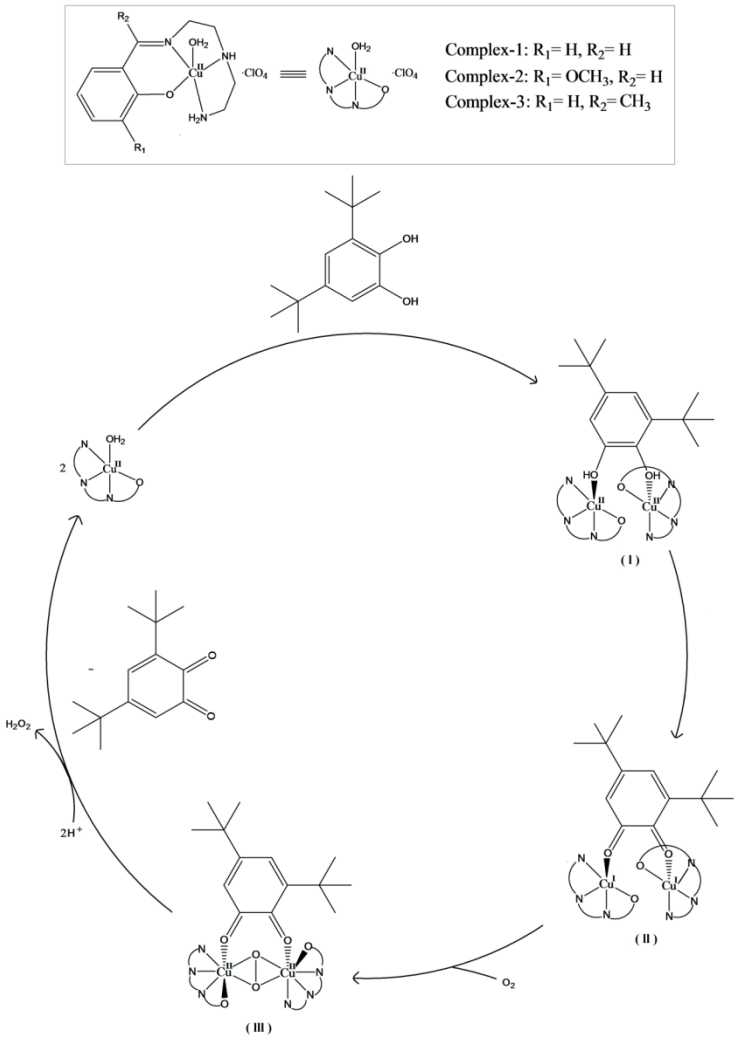

Scheme 1S. Possible mechanism of 3, 5-DTBC oxidation.